TECHNICAL UNIVERSITY OF LIBEREC
Faculty of Mechanical Engineering

Modification of the mechanical system of the needle bar

Master Thesis

Study programme:	N2301 Mechanical Engineering
Study branch:	Machines and Equipment Design
Author:	**Rakesh Nag**
Thesis Supervisors:	Ing. Jiří Komárek, Ph.D. Department of Design of Textile Machine

Liberec 2021

TECHNICAL UNIVERSITY OF LIBEREC
Faculty of Mechanical Engineering

Master Thesis Assignment Form

Modification of the mechanical system of the needle bar

Name and surname: **Rakesh Nag**
Identification number: S18000447
Study programme: N2301 Mechanical Engineering
Study branch: Machines and Equipment Design
Assigning department: Department of Design of Textile Machine
Academic year: **2019/2020**

Rules for Elaboration:

1. Perform a search for needle motion mechanisms.
2. Design modifications of the mechanical system of the needle bar.
3. Create mathematical models describing dynamic behavior of designed mechanical system and compare with original solution.
4. Elaborate drawing documentation for selected parts.

Scope of Graphic Work: drawing documentation
Scope of Report: 45
Thesis Form: printed/electronic
Thesis Language: English

List of Specialised Literature:

[1] MEERKAMM, Harald, ed. *Technical Pocket Guide*. Germany: Schaeffler Technologies GmbH & Co. KG, 2014.
[2] AMBEKAR, Ashok G. *Mechanism and machine theory*. Delhi: PHI Learning Private Limited, 2007. Eastern economy. ISBN 978-81-203-3134-1.
[3] KOMÁREK, Jiří. Dynamic Model of the Mechanical System of the Needle Bar. *Advances in Mechanism Design II, Proceedings of the XII International Conference on the Theory of Machines and Mechanisms*. Liberec: Springer, 2016, vol. 44, s. 323-329. ISBN: 978-3-319-44086-6.

Thesis Supervisors: Ing. Jiří Komárek, Ph.D.
Department of Design of Textile Machine

Date of Thesis Assignment: October 30, 2019
Date of Thesis Submission: April 30, 2021

L.S.

prof. Dr. Ing. Petr Lenfeld
Dean

doc. Ing. Martin Bílek, Ph.D.
Head of Department

Liberec October 30, 2019

Declaration

I hereby certify, I, myself, have written my master thesis as an original and primary work using the literature listed below and consulting it with my thesis supervisor and my thesis counsellor.

I acknowledge that my bachelor master thesis is fully governed by Act No. 121/2000 Coll., the Copyright Act, in particular Article 60 – School Work.

I acknowledge that the Technical University of Liberec does not infringe my copyrights by using my master thesis for internal purposes of the Technical University of Liberec.

I am aware of my obligation to inform the Technical University of Liberec on having used or granted license to use the results of my master thesis; in such a case the Technical University of Liberec may require reimbursement of the costs incurred for creating the result up to their actual amount.

At the same time, I honestly declare that the text of the printed version of my master thesis is identical with the text of the electronic version uploaded into the IS/STAG.

I acknowledge that the Technical University of Liberec will make my master thesis public in accordance with paragraph 47b of Act No. 111/1998 Coll., on Higher Education Institutions and on Amendment to Other Acts (the Higher Education Act), as amended.

I am aware of the consequences which may under the Higher Education Act result from a breach of this declaration.

January 11, 2021 Rakesh Nag

ACKNOWLEDGEMENT

With utmost gratitude, I would like to extend my heartfelt appreciation and thanks to my supervisor, Ing. Jiří Komárek Ph.D. (Department of Design of Textile Machine) for his knowledge, tremendous support, and consecutive guidance for the successful completion of my thesis work. Also, I like to say thanks for giving me an opportunity to perform this thesis work and for providing me with valuable advice and information regarding the technologies at every point.

I would also like to thank Professor Ing. Jan Valtera Ph.D. (Department of Design of Textile Machine) for his help during my thesis work while working on the magnetic proposal.

I also like to say thanks to my entire department colleagues for their unending support and insights on the various technologies required to complete my thesis.

I also want to thank my friends for their support in my life, especially during my thesis time by giving confidence words.

Everything that I have done so far is with the blessings from my parents, I am very much grateful to them for having faith and confidence in me throughout this journey.

ABSTRACT

The work presented in this thesis deals with the needle bars mechanism of a sewing machine that uses the floating needle to produce a decorative hand stitch. By using two mechanical systems of needle bar a single-needle is passed through the materials for every stitch. The mechanical system of the needle bar performs a rectilinear reciprocating motion which was realised by the cam mechanism.

For the present competitive world, it is necessary to increase productivity but it leads a sewing machine to produce a high level of noise and vibration because of increasing its operating speed. Based on the previous experimental work it was found that the main contributor for vibration and noise is a cam mechanism. Also, the mechanical system of the needle bar can be modified to reduce noise and vibration with its increased operating speed.

In this thesis work, the mechanical cam mechanism is replaced by a preselected mechatronic system with linear servo-motor. By dynamic analysis, the behaviour of a mechanical system of the needle bar was examined. Later the result from this analysis was used to compare the dynamic analysis of the modified functional model.

A total of five various kinds of modification for needle bar were proposed and dynamic analysis was done for two picked proposals. First with vibration isolator by using compact wire rope isolator, later as vibration absorber by using two permanent magnets.

Modification with Compact wire rope isolator was done by considering standard isolator available in the market by using its characteristics prescribed by the company. For magnetic vibration absorber, the selection of magnet was done by considering force v/s distance characteristics derived by using FEMM 4.0 software. Later it was inserted into the functional model to conduct dynamic analysis. The dynamic analysis result shows a noticeable reduction in the vibrational loss by using both the proposed modifications.

KEYWORDS

Sewing machine, Decorative hand stitch, Floating needle, Noise reduction, Linear servo-motor, vibration isolator, Compact wire rope isolator, Vibration Absorber, Permanent magnets

ANOTACE

Tato diplomová práce se zabývá mechanismem předání jehly šicího stroje, který využívá systém plovoucí jehly k výrobě ozdobného stehu. Použitím dvou mechanických soustav jehelní tyče prochází jedna jehla materiálem při každém stehu. Mechanická soustava jehelní tyče koná přímočarý vratný pohyb, který je realizován vačkovým mechanismem.

V současném konkurenčním světě je nutné zvýšit produktivitu. To ovšem vede k tomu, že šicí stroj produkuje vysokou hladinu hluku a vibrací kvůli rostoucí provozní rychlosti. Na základě předchozí experimentální práce bylo zjištěno, že hlavní příčinou vzniku vibrací a hluku je vačkový mechanismus a samotná mechanická soustava jehelní tyče, kterou lze upravit za účelem snížení hluku a vibrací při vyšších pracovních rychlostech.

V této diplomové práci je vačkový mechanismus nahrazen řízeným mechatronickým systémem s elektrickým lineárním servomotorem. Pomocí dynamické analýzy se zkoumá chování mechanické soustavy jehelní tyče. Později je výsledek této analýzy použit k porovnání dynamické analýzy upraveného funkčního modelu.

Bylo navrženo celkem pět druhů modifikací jehelní tyče, z nichž byly dále vybrány a zpracovány dva návrhy. Pro tyto dna návrhy byla provedena dynamická analýza. První úprava využívala tlumič vibrací složený s kompaktního ocelového lanka. Druhá úprava využívá pro tlumení vibrací dva permanentní magnety.

V prvním případě bylo využito standardního kompaktního lankového izolátoru vibrací dostupného na trhu s předem známými charakteristikami předepsanými výrobní společností. V druhém případě byl výběr magnetu proveden na základě posouzení silové charakteristiky v závislosti na vzájemné vzdálenosti dvou magnetů, která byla stanovena pomocí softwaru FEMM 4.0. Získané charakteristiky byly vloženy do matematického modelu, jež prováděl dynamickou analýzu. Výsledky dynamické analýzy ukazují znatelné snížení vibrací při použití navržených úprav.

KLÍČOVÁ SLOVA

Šicí stroj, Dekorativní steh, Plovoucí jehla, Snížení hluku, Lineární servomotor, Izolátor vibrací, Kompaktní lankový izolátor vibrací, Tlumič vibrací, Permanentní magnet

CONTENTS

LIST OF FIGURES 11

LIST OF GRAPHS 12

LIST OF TABLES 14

LIST OF ABBREVIATIONS 15

LIST OF SYMBOLS 16

CHAPTER 1. Introduction 17

1.1. Literature review 17

1.2. Needle motion mechanisms 18

1.3. The main mechanism for needle movement 18

1.3.1. Slider crank centric mechanism 19

1.3.2. Slider crank eccentric mechanism 19

1.3.3. Scotch yoke mechanism 19

1.3.4. Multiple bar mechanism 20

1.3.5. Swing shaft mechanism 20

1.4. Mechanism for an additional movement of the needle 21

1.4.1. Mechanism with needle movement in an arc path 21

1.4.2. Needle mechanism for zigzag sewing 22

1.4.3. Mechanism with needle swing in the sewing direction 22

1.5. Description of sewing machine DECO 2000 23

1.6. The existing needle bar mechanism 25

1.7. Detailed view of Needle bar 25

1.8. Problem in an existing sewing machine 26

CHAPTER 2. Aim of the thesis work 28

CHAPTER 3. Design of new functional model with linear servomotor 30

3.1. Construction of a new functional model 31

CHAPTER 4. Mathematical model of a new functional model with linear servomotor 34

4.1. Selection of the stroke function....34
4.2. Simulation setup for new functional model....37
4.3. Analysis result from new needle bar mechanism....38
CHAPTER 5. Proposal for modification to the needle bar....41
5.1. TRIZ method to find optimization....41
5.2. Cause and remedies for vibration in a system....42
5.3. Proposal used to reduce vibration in the needle bar of the mechanical system....43
5.3.1. Modification by using magnets....44
5.3.2. Modification by using an isolator....45
5.3.3. Modification by using a damper....46
5.3.4. Modification by using shock-absorbing metal....46
5.3.5. Modification in the design of the existing needle bar....46
5.4. Used modification from the above proposal....47
CHAPTER 6. Modification with wire rope isolator....48
6.1. Design modification of the functional model....49
6.2. Analysis for the modified functional model....50
6.3. Result comparisons....54
CHAPTER 7. Modification with permanent magnets....57
7.1. Selection of suitable magnets....58
7.2. Design modification of the functional model....60
7.3. Analysis for the modified functional model....62
7.4. Result comparisons....69
CHAPTER 8. Conclusion and discussion....72
REFERENCES....74
APPENDIX 1: New modified functional model with linear servomotor (Manufactured and Assembled model)....78
APPENDIX 2: Detailed view of the modified functional model with linear servomotor (Manufactured and Assembled model)....79

APPENDIX 3: Example of a Lua script written for FEMM 4.2 software to find the Force v/s Distance characteristics curve for a selected magnetic pair.....79

APPENDIX 4: Magnetic analysis result obtained from the FEMM 4.2 software for a written script.....85

APPENDIX 5: Critical damping value calculation for compact wire rope isolator. 86

APPENDIX 6: Magnetic force calculation.....86

APPENDIX 7: Proposed Modified Magnetic Vibration Absorber.....87

APPENDIX 8: Drawing documentation.....88

LIST OF FIGURES

Figure 1.1: Slider crank centric mechanism [7] 19
Figure 1.2: Slider crank eccentric mechanism [7] 19
Figure 1.3: Scotch yoke mechanism [7] 20
Figure 1.4: Multiple bar mechanism formed by crank mechanism and four-bar mechanism [7] 20
Figure 1.5: Swing shaft mechanism [7] 21
Figure 1.6: Mechanism with needle movement in an arc path [7] 22
Figure 1.7: Needle swing mechanism crosswise to the sewing direction [7] 23
Figure 1.8: Sewing machine DECO 2000 [4] 23
Figure 1.9: Types of decorative stitches [4] 24
Figure 1.10: Floating needle [7] 24
Figure 1.11: Floating needle for an upper needle bar [4] 24
Figure 1.12: Area of applications of decorative stitches [4] 24
Figure 1.13: Mechanism of a needle bar in DECO 2000 [7] 25
Figure 1.14: Cross-section of the mechanical system of the needle bar [7] 26
Figure 3.1: New functional model with linear servomotor 32
Figure 3.2: Detail view of a new functional model 33
Figure 4.1: Comparison of selected stroke function [12] 36
Figure 4.2: Comparison of the first derivative of the selected stroke [12] 37
Figure 4.3: Comparison of the second derivative of the selected stroke function [12] 37
Figure 4.4: Simulation set up for new functional model 38
Figure 5.1: Modification of needle bar using magnets 44
Figure 5.2: Compact wire rope isolator [25] 45
Figure 5.3: High energy rope mounts [25] 45
Figure 5.4: Modification of needle bar using wire rope isolator 45
Figure 6.1: Passive isolation system [20] 48
Figure 6.2: Detailed view of the modified functional model with WRI 49
Figure 6.3: Simulation set up for modified functional model with WRI 51
Figure 7.1: Magnets with the same width and with increasing height 59
Figure 7.2: Magnets with the same volume 59
Figure 7.3: Detail view of the modified functional model with permanent magnets 61
Figure 7.4: Simulation set up for modified functional model with permanent magnets 63

LIST OF GRAPHS

Graph 4.1: Position stroke function for complete sewing cycle [5] 35
Graph 4.2: Velocity stroke function for complete sewing cycle [5] 35
Graph 4.3: Acceleration stroke function for complete sewing cycle [5] 36
Graph 4.4: Position curves comparisons between input stroke and output response 39
Graph 4.5: Velocity curves comparisons between input stroke and output response 40
Graph 4.6: Acceleration curves comparisons between inputs stoke and output response 40
Graph 6.1: Characteristics curve for a selected wire rope isolator [25] 50
Graph 6.2: Position comparison between input stroke and output response for a modified model with WRI 52
Graph 6.3: Velocity comparison between input stroke and output response for a modified model with WRI 53
Graph 6.4: Acceleration comparison between input stroke and output response for a modified model with WRI 53
Graph 6.5: Position comparison between input stroke, the output response of the modified model with WRI and with the original unmodified model 54
Graph 6.6: Velocity comparison between input stroke, the output response of the modified model with WRI and with the original unmodified model 55
Graph 6.7: Acceleration comparison between input stroke, the output response of the modified model with WRI and with the original unmodified model 56
Graph 7.1: Force v/s Distance curve for different magnets of the same size 58
Graph 7.2: Force v/s Distance curve for magnets with the same width and by increasing height 60
Graph 7.3: Force v/s Distance curve for magnets with the same volume 60
Graph 7.4: Force-distance characteristics for a selected magnet 62
Graph 7.5: Sensitivity analysis for magnets of same base width 64
Graph 7.6: Sensitivity analysis for magnets of the same volume 65
Graph 7.7: Sensitivity analysis of magnets 65
Graph 7.8: Position comparison between input stroke and output response for a modified model with permanent magnets 68
Graph 7.9: Velocity comparison between input stroke and output response for a modified model with permanent magnets 68

Graph 7.10: Acceleration comparison between input stroke and output response for a modified model with permanent magnets.....69
Graph 7.11: Position comparison between input stroke, the output response of the modified model with permanent magnets and with the original unmodified model.....69
Graph 7.12: Velocity comparison between input stroke, the output response of the modified model with permanent magnets and with the original unmodified model.....70
Graph 7.13: Acceleration comparison between input stroke, the output response of the modified model with permanent magnets and with the original unmodified model 71

LIST OF TABLES

Table 6.1: Kinetic energy comparison between the models 55
Table 7.1: Maximum velocity during impact for different square cross-sectioned magnet 66
Table 7.2: Kinetic energy comparison between the models 70

LIST OF ABBREVIATIONS

DECO 2000	-Decorative hand stitching machine
AMF	-American Machine and Foundry Company
dB	-Decibels
RPM	-Revolutions per minute
SPM	-Stitches per minute
TRIZ	-The Theory of inventive problem solving
NIB	- Neodymium Magnet
WRI	-Wire Rope Isolator
CWRI	-Compact Wire Rope Isolator
HERM	-High Energy Rope Mount
PWRI	-Polycal Wire Rope Isolator
HWRI	-Helical Wire Rope Isolator
MR Damper	-Magneto-Rheological Damper
MS Office	-Microsoft office
FEMM	-Finite Element Method magnetics
DVA	-Dynamic Vibration Absorber
MVA	-Magnetic Vibration Absorber
MMVA	-Modified Magnetic Vibration Absorber
QZS	-Quasi Zero Stiffness

LIST OF SYMBOLS

β	-cam angle (rad)
h,x	-Displacement(m)
v	-Velocity (m/sec)
a	-Acceleration (m/sec^2)
t	-Time (sec)
m	-Mass (kg)
F	-Force (N)
P	-Momentum (kg.m.s^{-1})
ρ	-Density (kg.m^{-3})
E_k	-Kinetic energy (J or kg.m^2 s^{-2})
C	-Damping coefficient (N.s.m^{-1})
K	-Stiffness coefficient (N.m^{-1})

CHAPTER 1. Introduction

1.1. Literature review

The history of Sewing or stitching was started in the Paleolithic era. According to human history, Sewing's concept came from the stone age when people started joining two-piece of animal skin using a needle made of bones and ivory to protect themselves from the changing environment **[1].**

Later the low productive manual Sewing started converting to machine sewing. In 1755 by german engineer Charles Fredrick Wiesenthal invented double pointed needle with an eye at one end was awarded a British patent for his work. Later in 1790 by English inventor, Thomas Saint got the first-ever patent for a complete sewing machine using chain stitch. The first-ever functional sewing machine was invented by a French tailor by Barthelemy Thimonnier in 1830 and awarded a French patent for his work. Later in 1834, Walter Hunt invented the first successful lockstitch sewing machine, and in 1851 an American inventor Allen Benjamin Wilson developed a rotary hook for a lockstitch sewing machine that started dominating others because of its silent and smooth running operation **[2]**, **[3].**

In today's competitive world it is necessary to run the sewing machine quieter, long-running with a reduction in vibration and shock to increase productivity. The same issues were solved in this thesis dealing with a new mechanism of needle bar of decorative sewing machine DECO 2000 using a floating needle with two mechanical systems of needle bar transfer needle each other. DECO 2000 is the first fully programmable electric eyelet buttonhole machine from AMF Company developed in 2003 **[4]**.

Pejchar was worked on the analysis and optimization of the dynamic behaviour of sewing machine DECO 2000. He measured the sound intensity in the sewing machine along with acceleration on the selected control part to reduce vibration and noise from the available needle bar mechanism. Later the modification on the available cam was done to reduce the evenness of the cam. He concluded with a note of changing the available sinusoidal cam to another cam form **[5]**.

Beran et, al were worked on an experimental analysis of a sewing machine to measure the behaviour of the sewing mechanism. They carried out the mapping of sound intensity in the area around the sewing machine to locate the intensity of a source of impact loading and found the maximum sound power of 83.6 dB at the operating speed of 250 RPM at the

covered stage in a sewing machine. Along with this analysis with the measured acceleration value on the needle bar, they concluded that the cam mechanism is the maximum contributor of noise and vibration in the sewing machine **[6]**.

Komarek was worked on the needle bar mechanism of a sewing machine. In his work, he replaced the mechanical cam mechanism with a mechatronic rotary servo motor where individual synchronous servo motor drives the mechanical system of the needle bar separately by using a belt mechanism to provide the desired movement for needle bars. He also proposed modifications for needle bar to reduce noise and are tested experimentally as well **[7]**.

1.2. Needle motion mechanisms

The sewing needle movement mechanism must meet all the requirements for proper stitching. The movement of the needle being linked to the other sewing machine mechanisms involved in the stitching process. The sewing needle held in the needle bar pierces the sewn material. In its return movement, a loop is formed from the upper thread guided by the needle, picked up by the tip of the hook or other loop-catching device. The needle performs a linear reciprocating movement either in a straight or an arc path. This movement can be called the main movement. For various sewing methods, the needle should have other movements as well. Supplementary needle movement allows both the needle injection site to be changed, for example by swinging the needle bar guide, and secondly, to change the position of the suture material guide through the needle handle by rotating the needle bar about its axis. The requirements for the movement of the individual parts of the mechanism resulting from the needle movement mechanism's said function. These movements are allowed by various articulated or cam mechanisms. Some sewing machines have only the mechanism of the main needle movement; in others, the mechanisms of one or more complementary movements work simultaneously. Mechanisms of needle movement have undergone many years of development, so it is impossible to cover all kinds and solutions fully.

1.3. The main mechanism for needle movement.

The needle performs a linear reciprocating movement either in a straight or an arc path to stitch the material. The following stated mechanism can perform the rectilinear reciprocating movement which is a part of the needle bar mechanism.

1.3.1. Slider crank centric mechanism

In most of the primary sewing machines, the needle performs a reciprocating movement. This main needle movement is most often provided by a crank mechanism allowing the rotational movement to be converted into a linear reciprocating movement. As it can be seen in figure 1.1, crank 2 connected to the motor shaft that performs a rotational movement, it can be transmitted through the connecting rod 3 to the needle bar 4 which is a sliding mounted to frame 1. The connecting rod with the crank and needle bar is secured by pin connection.

1.3.2. Slider crank eccentric mechanism

The eccentric crank mechanism can be seen in figure 1.2 that the center of rotation of the crank is located outside the axis of movement of the needle bar. Their relative position is indicated by eccentricity 'e'. The motor shaft is connected to crank 2 which is connected to connecting rod 3 that transfer the motor shaft's rotational motion to the needle bar linear reciprocating motion. Here needle bar 4 acts as a slider in a slider-crank eccentric mechanism.

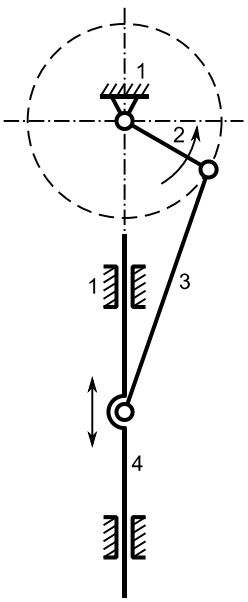

Figure 1.1: Slider crank centric mechanism [7]

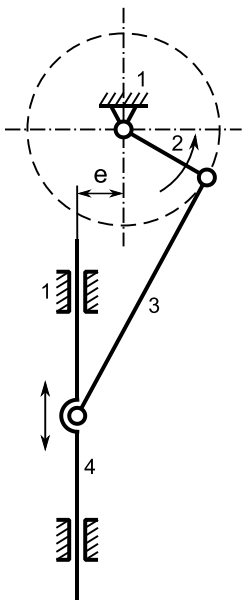

Figure 1.2: Slider crank eccentric mechanism [7]

1.3.3. Scotch yoke mechanism

The Scotch Yoke mechanism is a reciprocating motion mechanism, converting the rotational motion of a crank 2 to linear motion of the needle bar 4. The needle or other reciprocating part 4 is directly coupled to a sliding yoke 3 with a slot that engages a pin P on the rotating part. The piston's location versus time is simple harmonic motion, i.e., a sine wave having constant amplitude and constant frequency, given a constant rotational speed. The scotch yoke mechanism is shown in figure 1.3

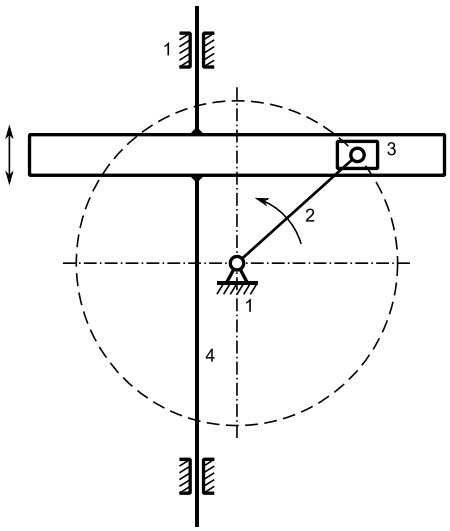

Figure 1.3: Scotch yoke mechanism [7]

1.3.4. Multiple bar mechanism

The Multiple bar mechanism is shown in figure 1.4 consists of a primary four bar-hinge mechanism with members 1, 2, 3, 4, to which a binary group 5, 6 is attached. 4, 5, 6 forms an eccentric crank mechanism. Mechanism 1, 2, 3, 4 act as a crank, 5 will be the connecting rod connected to the needle 6 to perform the linear reciprocating motion.

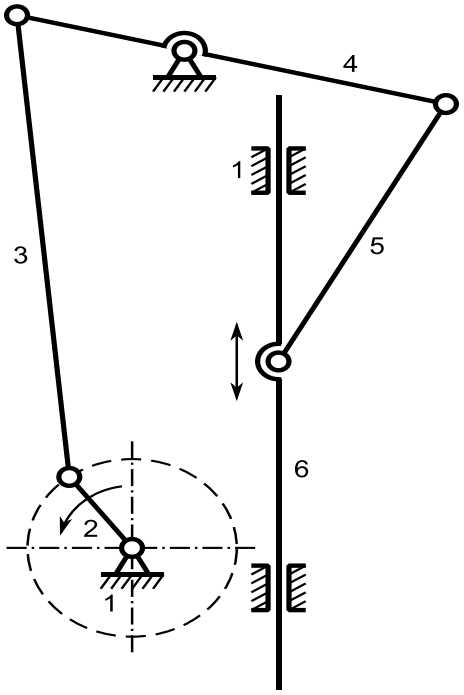

Figure 1.4: Multiple bar mechanism formed by crank mechanism and four-bar mechanism [7]

1.3.5. Swing shaft mechanism

The swinging mechanism can also provide the required needle movement. The principle is the same as that of a multiple bar mechanism. The rocking shaft 1 is located in the upper

part of the machine frame parallel to the lower main shaft 2. At both ends, it is terminated by levers 3, 4. The right lever movement comes from the main shaft eccentric 5 via the connecting rod 6. The motion transfer to the needle bar 8 through a small connecting rod 9, and the connecting lever 7 makes the needle move in a linear reciprocating motion. Figure 1.5 shows the modelled swing shaft mechanism.

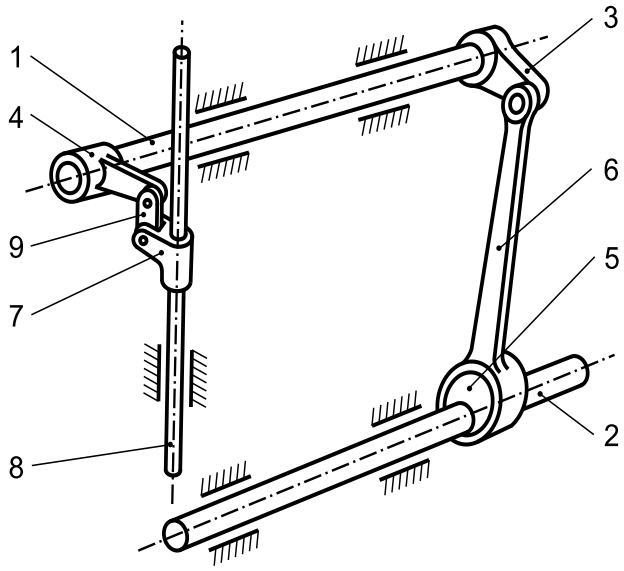

Figure 1.5: Swing shaft mechanism [7]

1.4. Mechanism for an additional movement of the needle

As mentioned in the above section, the needle performs a linear reciprocating movement in a straight can be called a main (primary) movement. The below mentioned mechanisms perform an additional movement that necessary for sewing decorative stitches which can also be called secondary movement.

1.4.1. Mechanism with needle movement in an arc path

The arc path mechanism is used for circular reciprocating needle movement shown in figure 1.6. The main part is formed by a four-bar mechanism 1, 2, 3, 4, to which the binary group 5, 6 is attached. The four-hinge mechanism is a crank arm with a rocker arm 4. The needle is clamped in the bracket on the rocker arm 6 through a connecting rod 5.

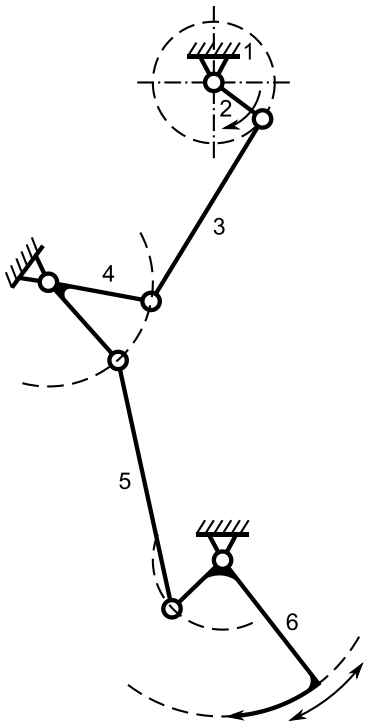

Figure 1.6: Mechanism with needle movement in an arc path [7]

1.4.2. Needle mechanism for zigzag sewing

In an additional movement to the main movement, the needle should move in sideways in a plane perpendicular to the feed direction to achieve the zigzag stitches. The needle must be moved to an extreme position for the wide grooves while moving over the material: otherwise, the needle will bend. Several types of holders allow achieving the swinging movement of the needle. These are set in motion utilizing four-joint or cam mechanisms. A basic diagram of one of the needle bar movement mechanisms with additional movement is shown in figure 1.7. The main movement of the needle bar 5 generates by the crankshaft 7. The secondary rocking movement is derived from the rotational movement of crank 2 via the four-hinge mechanism 1, 2, 3, 4 on the needle bar guide 4. Crank 2 is driven by the main shaft 7 via gears A and B with a gear ratio of 1:2.

1.4.3. Mechanism with needle swing in the sewing direction

This mechanism provides the needle bar to perform both the primary and secondary movements similar to the previous mechanism. It uses the principles described above for zigzag motion. Here, the needle is pivoted in the sewing direction after insertion into the material, thereby allowing a good feeding of both sewn material layers. In this method needle feed and works in conjunction with the bottom-feed.

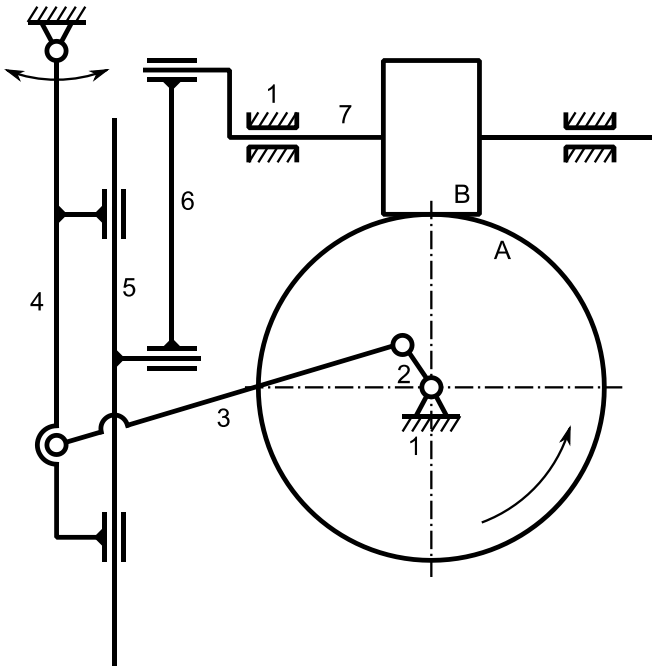

Figure 1.7: Needle swing mechanism crosswise to the sewing direction [7]

1.5. Description of sewing machine DECO 2000

The decorative hand stitching sewing machine DECO 2000 is shown in figure 1.8 can duplicate the work made by a skilled hand sewer by sewing perfect pick stitch, saddle stitch, and a saddle stitch with a long or short variation stitch as shown in figure 1.9**[4].**

Figure 1.8: Sewing machine DECO 2000 [4]

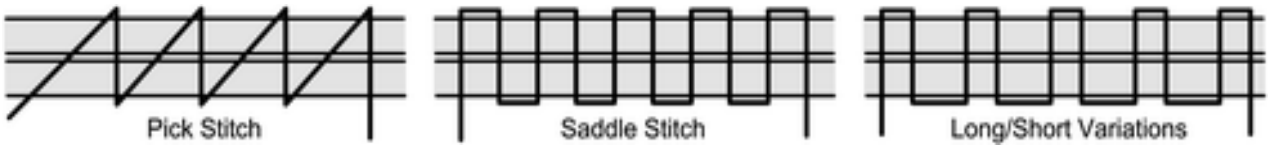

Figure 1.9: Types of decorative stitches [4]

A floating needle is used as a needle in a decorative hand stitching sewing machine, which is a double-pointed needle with an eye in the center as shown in figure 1.10. The needle is transmitted through the material to be sewn. Two-needle bars of a mechanical system are working one above and one below the worktable of the machine, the needle then passes through the material in each stitch. The floating needle held in a mechanical system, getting a transfer from the upper needle bar to the lower needle bar, refer the figure 1.11.

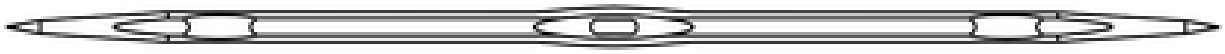

Figure 1.10: Floating needle [7]

Figure 1.11: Floating needle for an upper needle bar [4]

These stitches had a wide variety of applications, mainly for decorative purposes. Typical applications are in men's and Ladies tailored jackets, Suits, Overcoats, Leatherwear, Ladies blouses, and in the Automobile industry. Some fields of application of the decorative stitches are shown in figure 1.12.

Figure 1.12: Area of applications of decorative stitches [4]

1.6. The existing needle bar mechanism

The mechanism of the existing needle bar is shown in figure 1.13. The mechanical system of needle bar 1 reciprocates rectilinearly which is realised by cam mechanism 2 over lever arm 3. The radial groove cam is common to both the mechanical system of the needle bars, which is driven by an asynchronous motor via the V belt. The Machine mean speed of the cam is varies from 75 to 250 RPM that corresponds to 150 to 500 SPM.

The lever arm 3 is mounted on the shaft 4 of a two-armed lever. The one-armed end is mounted with roller 6 through lever arm 3, which moves in a radial groove of the cam along its active surface, which gets the input as a circular motion. The other side of the armed end is mounted with a guiding gate 8 through lever arm 7 that makes the needle bar to move in a rectilinear reciprocating motion. The needle bar movement gets protected with two sliding bushes 9, 10 to reduce wear and prevent the needle bar from further damages. This entire mechanism system is mounted on machine frame 5. The complete mechanism with a two-needle bar arrangement is shown in figure 1.13.

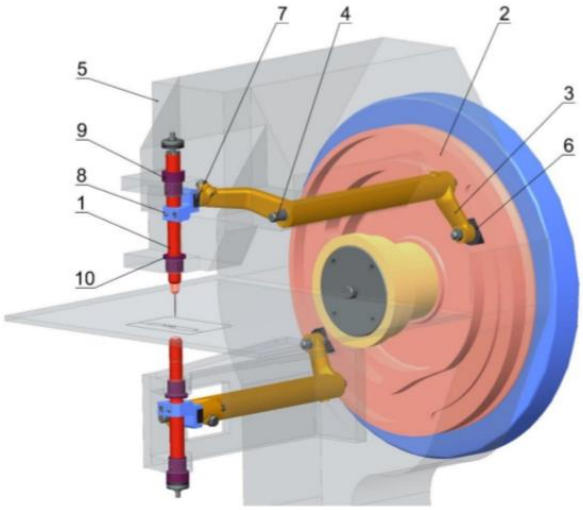

Figure 1.13: Mechanism of a needle bar in DECO 2000 [7]

1.7. Detailed view of Needle bar

The section view of the mechanical system of the needle bar is shown in figure 1.14. The floating needle 20 is held by the gripper having two balls 12 within the mechanical system of the needle bar. The gripper is made up of two steel balls whose axial movement is controlled by cylinder 4. The balls are pushed into a tapered conical hole in shell 2 because of spings 11,15 pressing force during shell 2 movements.

The needle release started once the control part (moving parts) of the needle bar get collides with the needle bar machine frame with sliding block bushes 18 shown in figure 1.14(b). The rubber pad 10 helps to absorbed impact force after the collision. The rubber pad movement got restricted by rubber pad support 17 with a threaded nut 16 during a collision. Needle bar shell 2 continues in the movement towards the bottom dead center position after impact also which helps the balls to release into a conical hole.

Shaft 3 helps to hold the rubber pad in one hand and on the other hand shaft end 6 helps in a movement of cylinder 4 with the help of spring 15. The shaft movement is guided by shaft guide 9. The spring 11 is also mounted in this shaft 3. The motion of the needle bar is realised by the cam mechanism through guiding supports 7, 8 through a two-armed lever, which is explained in the above section 1.6 **[9]**.

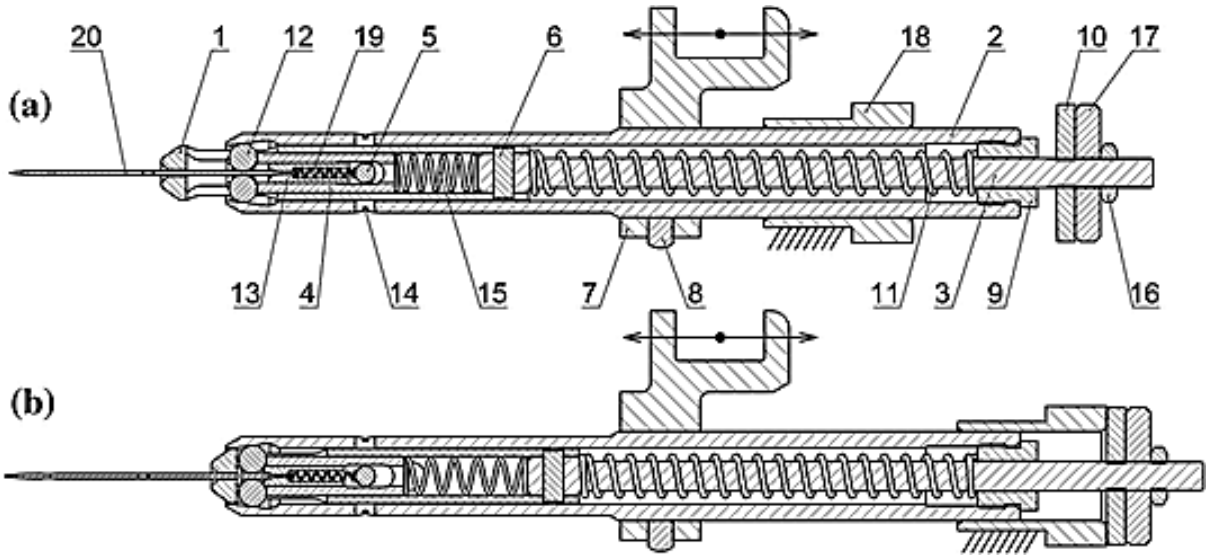

Figure 1.14: Cross-section of the mechanical system of the needle bar [7]

a. Needle holding position b. Needle release position

1.8. Problem in an existing sewing machine

The current existing sewing machine operation mode is from 150 to 500 SPM. At present, the machine operates at 380 SPM, but the operator wants to shift it to 500 SPM to increase productivity. Achieving the required speed is difficult because of the higher dynamic force acting on the machine and the system starts vibrating once it achieves the same **[10]**. Hence there is a vibrational and high noise level problem in an existing sewing machine, which is terrible for the machine and the worker as well.

High vibration in a machine reduces the lifetime of the machine and influences badly on human health by creating a negative effect on the human organism by reducing the performance of a person's ability to focus on activity. Therefore it is necessary to protect people from excessive noise and shock. Protection can usually be done by removing undesirable vibration, noise, and shock from the system.

At higher speed due to the large dynamic lead to excessive wear of system components like needle will negatively impact the system life. Due to frequent shutdown to repairs at risk can cause a delay in productivity.

Cam mechanism is the primary source of vibration and noise. So it is better to replace the cam mechanism with other mechanisms with an electric drive. The mechanical modification of the available functional model with rotary servomotor was done earlier **[7]** and with the pre-selected linear servomotor new modification was done to the functional model and is dynamically verified which is described in detail in the next chapters. The mathematical model describes the dynamic behavior of the mechanical system of the needle bar without the influence of the cam and gear mechanisms. These results were used to compare the modified needle bar system's behaviour, which was the main aim of this thesis work.

CHAPTER 2. Aim of the thesis work

The existing cam mechanism is driven by an asynchronous motor that transfers rotational motion to the reciprocating linear movement of the needle bar through a multimember mechanism. Experimental analysis shows the presence of high levels of noise and vibration on the decorative sewing machine, which was operated by a cam mechanism **[6]**. A high level of noise and vibration from the machine will not affect only the machine but it may also affect human health that used to working with it. So it is necessary to take extra care to solve it. The existing radial cam mechanism should get replaced with a mechatronic system with electric actuators. The electrical servo drive is the best outcome from the choice to replace the mechanical radial cam. So mechanical cam get replaced to electric cam operated with suitable positional feedback. The modification of the functional model with the linear servo drive was done and it is described in detail in the next chapters. Also from the dynamic analysis of the new functional model with linear servomotor states that the other reason for the noise and vibration in a functional model is the impact of the rubber pad on the needle bar machine frame. So it is necessary to reduce loss by kinetic energy to reduce vibration on the functional model with a linear servomotor, without compromising the functionality of the needle bar mechanism.

The main aim of this thesis work is to perform a modification on the existing mechanism of the needle bar, which would replace the existing unsatisfactory solution that leads to a reduction of noise and vibration on the sewing machine. Available radial cam mechanical system allows the sewing machine to operate in the range between150 to 500 SPM and the machine will be working at 380 SPM but the manufacturer wants to increase it to 500 SPM to enhance productivity. The main parameter expressing the productivity in the sewing machine is by a sewn quantity which is stitches per unit time (SPM-Stitches per minute). The speed of the needle bar is the main parameter to control the sewn quantity. It is necessary to allow the mechanical system to raise its needle bar operating speed to increase its productivity. The newly modified mechanism of the needle bar must enable it to run smoothly even at a higher operating speed (250 RPM), leading to an increase in productivity.

To test the optimization of the newly designed modified mechanism with the electric cam of linear servomotor, modification on the existing functional model is necessary. However, it should reach the existing mechanism specification to make it functional. Also, testing on the functional model will be more flexible and able to reduce the testing cost compared to do it directly on the sewing machine.

The thesis's main objective is to reduce noise and vibration from the decorative sewing machine and to reduce unnecessary vibrational force, and shock during impact between the rubber pad and the needle bar machine frame. In the meantime, it helps to improve the life span of the needle bar, make an easy operation during working. So if it can achieve all these objectives then it is possible to raise the operating speed of the machine without any vibration problem which leads to an increase in production, and both sewn quality and quantity.

CHAPTER 3. Design of new functional model with linear servomotor

As mentioned in the last chapter that the existing model uses a cam mechanism to convert the rotational motion of a single electric drive to the reciprocating linear motion of a needle bar. The single electric drive should control both the needle bar movement, which leads to a series of drawbacks. The Cam mechanism should replace the electric drive since the cam mechanism is the main source for vibration and noise generation in the model **[6]**. So it is necessary to change the functional model from the mechanical cam to the electrical cam, it does reduce vibration and shock and simplifies the design of the functional model as well.

Changing the model from a mechanical cam mechanism to a mechatronic system with electric actuators leads to choosing the better electric drive type that suits the system's current operational mechanism. Electric servo drive control provides a proper working position for actuator mechanism, which uses electrical energy and converts it into mechanical work. The drive with active feedback helps the actuator's endpoint to increase its accuracy and control speed when needed. The electric servo drive is a better option than any other type of drive in terms of functionality and serviceability.

The servo drive consists of a power and control unit, where the power unit consists of electric motors, power converter, and their accessories, and the control unit consists of the control electronics circuits. The replacement of the mechanical cam mechanism to a rotary servo motor with a gear mechanism was done before **[7]**. The new functional model with pre-selected linear servomotor was designed to conduct dynamic analysis. The linear servo motor used in the current design will work as an electromagnetic drive. It consists mainly of two parts as the slider and the stator. The slider will be inside the stator. The slider is made of series of neodymium magnets that are mounted inside a highly precise Stainless Steel tube. The stator contains the motor windings, bearings, position and temperature sensors, and a microprocessor unit for monitoring the motor. The slider and the stator are placed and guided by the linear guide. They help to provide high precision guidance and allow the load to be dynamically and precisely positioned. The load is mounted directly onto the front plate of the linear guide **[11]**.

3.1. Construction of a new functional model

Implementing the newly designed model directly into the original machine makes no sense without verifying its functionality and its reliability. So it is necessary to create a functional model either the entire newly-designed mechanism or just its potentially most problematic part.

Construction of a newly designed functional model with needle bar and drive system was first done in the CREO PARAMETRIC 4.0 modelling tool. Later the functionality of the system was also checked in CREO PARAMETRIC 4.0 with the help of the mechanism tool, and it is described in detail in the further chapters.

Figure 3.1 shows the newly designed functional model with linear servomotor. It will help to convert linear motion from the electrical servo drive to the mechanical movement of the needle bar. As it showed in the figure, the functional model is attached to support plate 1 and it is attached to the rigid support frame 2 with massive clamping and with a suitable rubber bush for stands. Like the original sewing machine, the functional model also had the symmetrical arrangement of the mechanical system of the needle bar 3 and every needle bar motion is powered by its own synchronous linear servomotor 4. Detail view of the functional model with drive, needle bar, and a connecter is shown in figure 3.2.

The needle bar is mounted on the rigid needle bar machine frame 5 to support its movement; the frame opening will be having sliding bushes 6 on both the end to eliminate direct contact between the needle bar and machine frame. Linear servomotor was connected to the needle bar through a mechanical connecting part 7 using suitable mechanical fasteners. The guiding gate 8 was connected to the connecting part through a suitable mechanical retaining Seeger ring. So the input motion from the drive will transfer through the connecting part and make the needle bar to move in a desired prescribed motion.

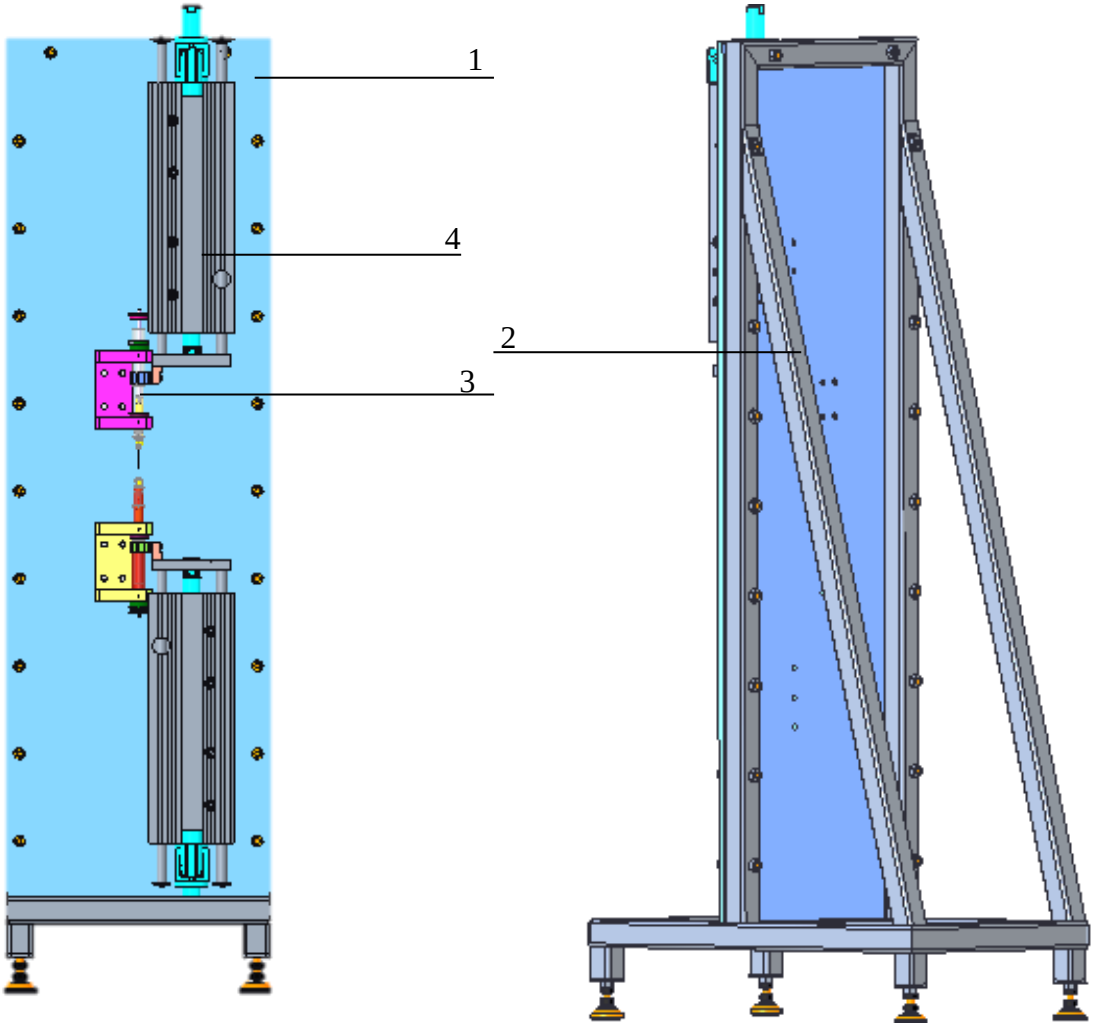

Figure 3.1: New functional model with linear servomotor

The spindle or slider of the linear servomotor 9 is the source for the movement in a drive. Spindle moves in the desired prescribed motion set by the control unit of the drive. The linear servo motor works by passing an electric current to the spindle by producing a magnetic field in it. The alternative attraction and repulsion by the spindle make it to move in the linear direction. The servo motor is a closed-loop system that incorporates position feedback to control the system's linear speed and position. So the desired motion from the drive is given utilized in the electrical form will control the needle bar separately, making it an electrical cam rather than a mechanical cam, which controls the complete process from a single motor.

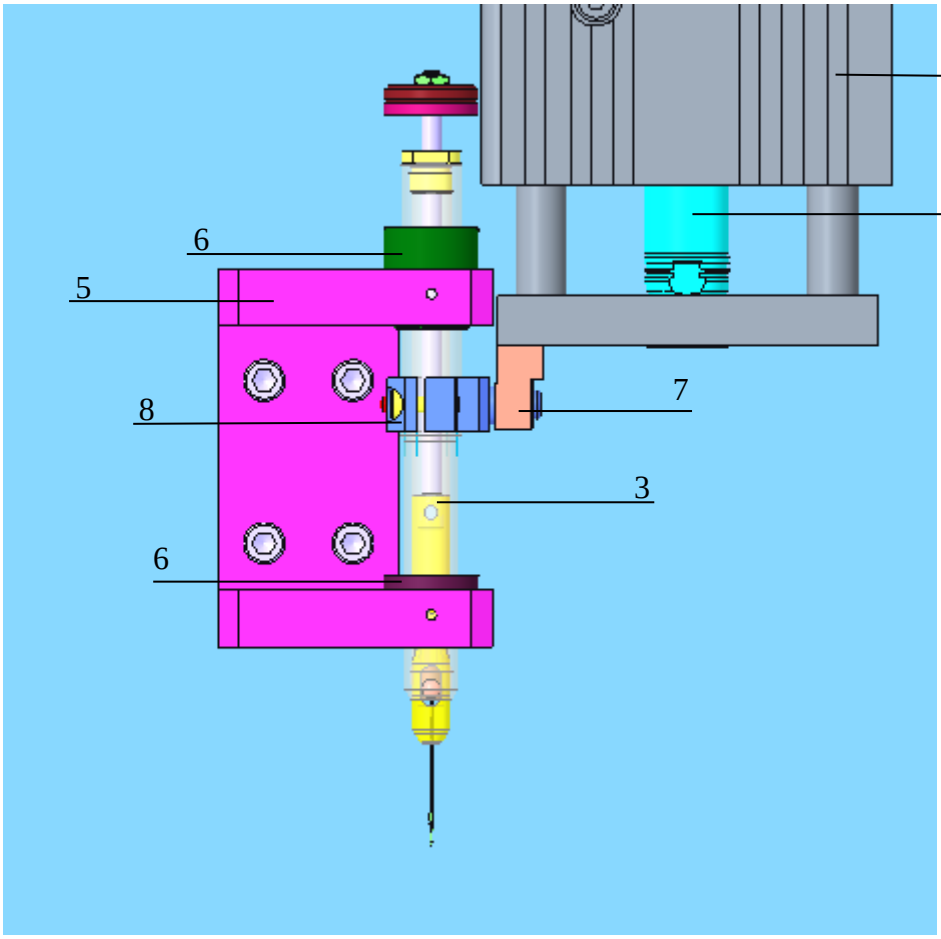

Figure 3.2: Detail view of a new functional model

The main advantage of using an individual drive to operate each needle bar is to make the functional model more flexible over the design. This helps to modify the functional model to more advance according to the latest industrial requirement. As mentioned before the main reason to achieve modification is to make the sewing machine work more smoothly with an increase in its productivity and lifespan.

The dynamic analysis for the current state of the needle bar with linear servomotor is performed and the results were compared with the proposed modification of the needle bar. The next chapter described the mechanical simulation for the current needle bar, and the analysis results were explained at the end of the chapter.

CHAPTER 4. Mathematical model of a new functional model with linear servomotor

The needle transfer mechanism is a part of a sewing machine of the functional model that can imitate the handmade stitch. It is necessary to ensure the floating needle transfer between two operating needle bars one above and below the machine bed on the supporting plate of the functional model. As mentioned before the needle bar perform a rectilinear reciprocating movement, which will be realised by the linear servo drive with suitable stroke function in the newly modified functional model.

The suitable stroke function was defined and inserted into the newly designed functional model with a linear servo motor. Later the dynamic analysis was performed for an applied stroke in CREO PARAMETRIC 4.0 by using the mechanism simulation tool. The response was extracted and compared with the input stroke function in an excel sheet. This chapter is about selecting a suitable stroke function and the result comparison and the conclusion about the modified functional model.

4.1. Selection of the stroke function

The complete sewing cycle is the needle bar's movement from top dead position to bottom dead position of both the needle bar that includes the transfer of needle from one needle bar to another. The complete sewing cycle is defined by an angle of rotation of 2π or 360^{o}, but the response is symmetric so it is enough to introduce just a part of the stroke that transfers the needle from one needle bar to another needle bar to the functional model for the dynamic analysis. The stroke responsible for transferring the needle from the one needle bar to the other needle bar is 60^{o} which can be named as an onward movement. Then there is a rest period of 180^{o} again the transfer of the needle back to the first needle bar will be by 60^{o} called a backward movement followed by a second rest period of 60^{o}. The displacement curve about this stroke for the lower needle bar is shown in the below graph 4.1. Furthermore, the corresponding velocity and acceleration curves are in graph 4.2 and 4.3 correspondingly **[5]**.

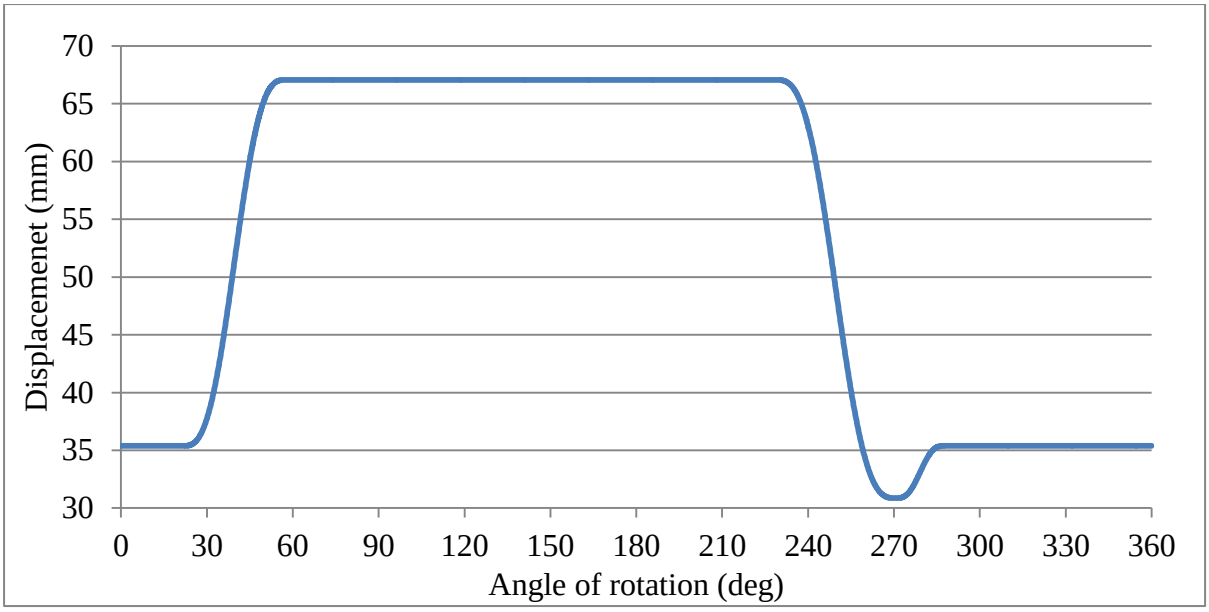

Graph 4.1: Position stroke function for complete sewing cycle [5]

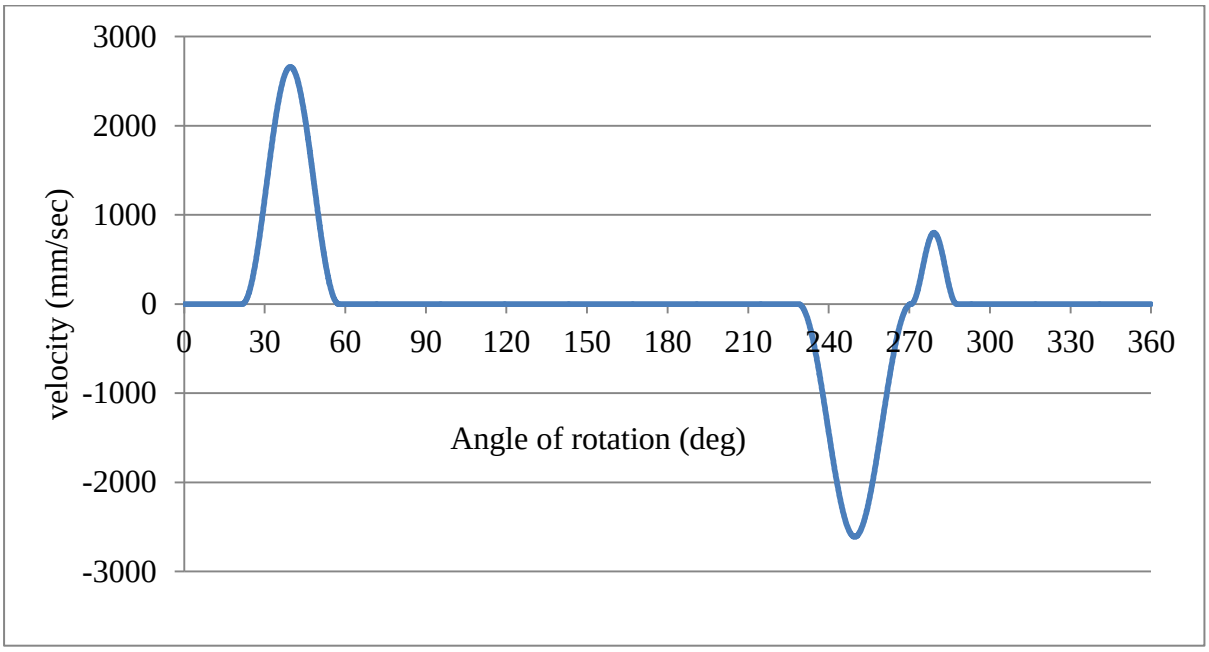

Graph 4.2: Velocity stroke function for complete sewing cycle [5]

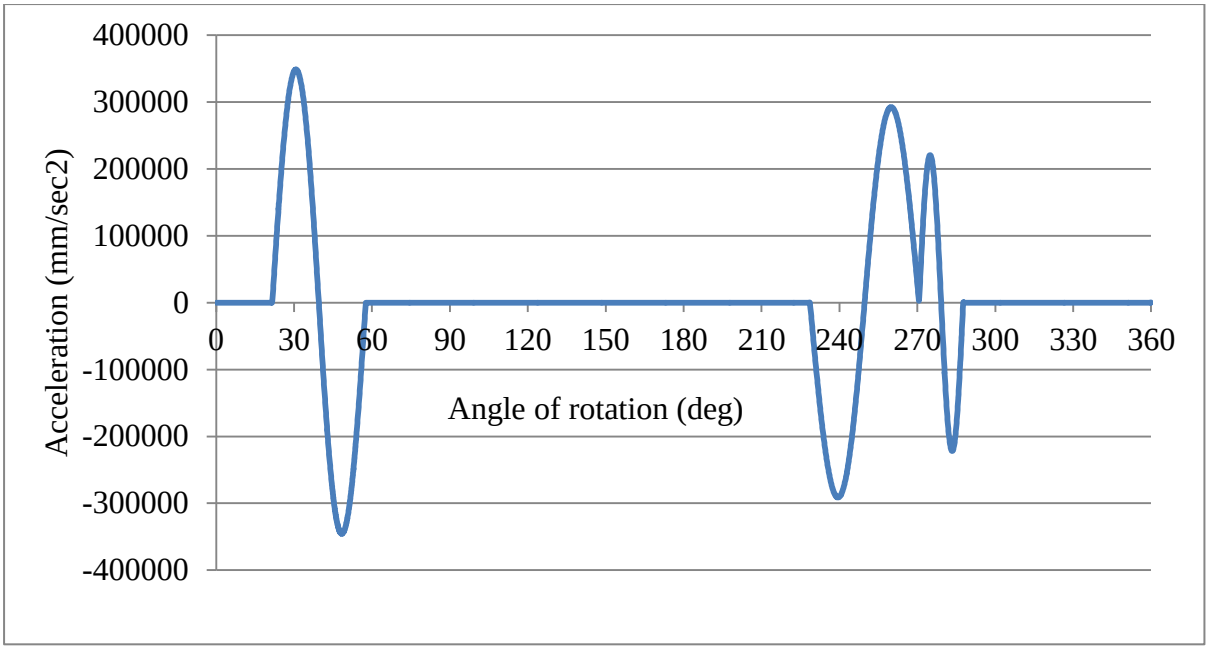

Graph 4.3: Acceleration stroke function for complete sewing cycle [5]

The functional model with linear servomotor uses a simple Cycloidal displacement (sine acceleration) function with an operating speed of 250 RPM with the working stroke of the needle bar is 32mm. The Cycloidal stroke function is the simplest type of stroke when compared to other stroke function. Figures from 4.1 to 4.3, shows the stroke function of Cycolidal, modified sinus, trapezoid along with the polynomial function for displacement, velocity, and acceleration. In the figure, the value of 'β' is 60º, equivalent to a time of 0.025sec. Moreover, the value of 'h' is equivalent to the stroke function of the needle that is the same as 32mm **[12]**.

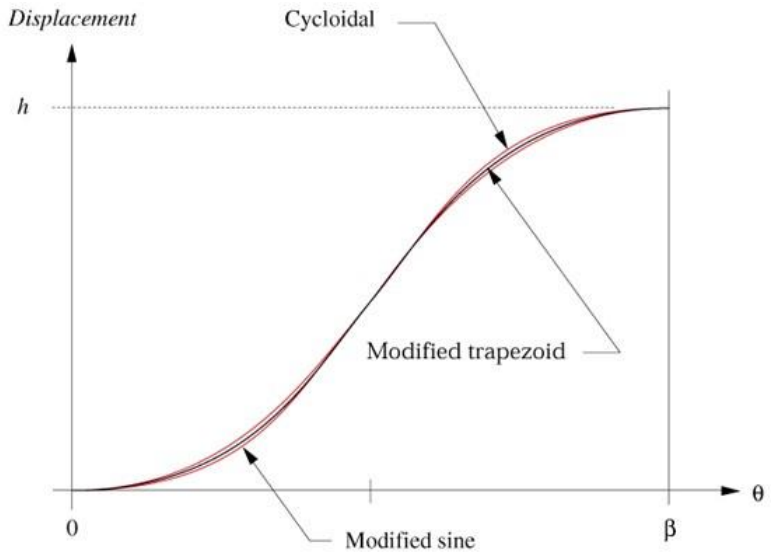

Figure 4.1: Comparison of selected stroke function [12]

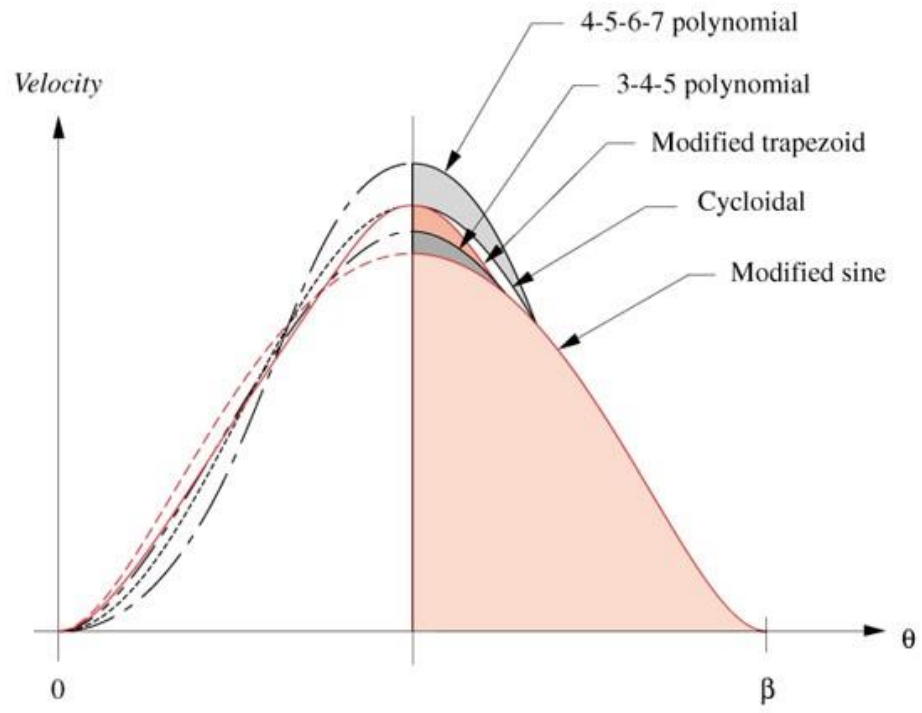

Figure 4.2: Comparison of the first derivative of the selected stroke [12]

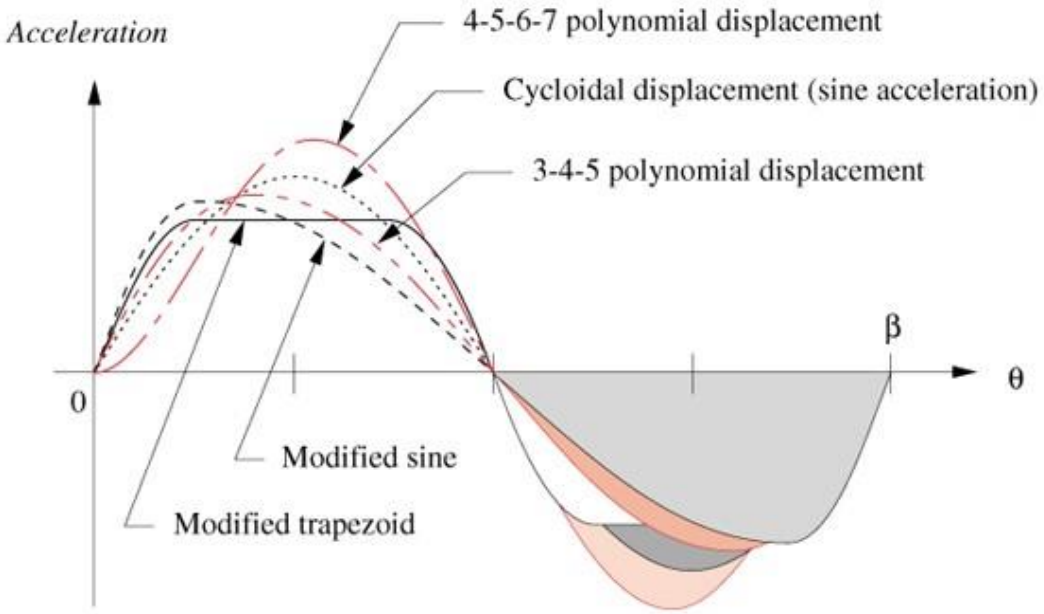

Figure 4.3: Comparison of the second derivative of the selected stroke function [12]

4.2. Simulation setup for new functional model

The dynamic analysis was conducted to analyse and compare the result with the input stroke. Figure 4.4 shows the simulation setup with the electric servo drive. Needle bar assembly was done with all necessary spring, damper, and with proper connections by using CREO PARAMETRIC 4.0 software. The corresponding values were inserted during the

analysis to the needle bar. The nonlinear stiffness of the rubber pad was experimentally determined. The obtained force curve acting on the pad depending on its compression was inserted into the model which is mentioned in figure 4.4. In the mathematical model, the damping value was simply described by the constant value which was chosen based on the real behaviour of the mechanical system of the needle bar. This behaviour was observed using a high-speed camera **[7]**. Then the mechanism was run in CREO the graphs were extracted and compared with the input strokes that were described below.

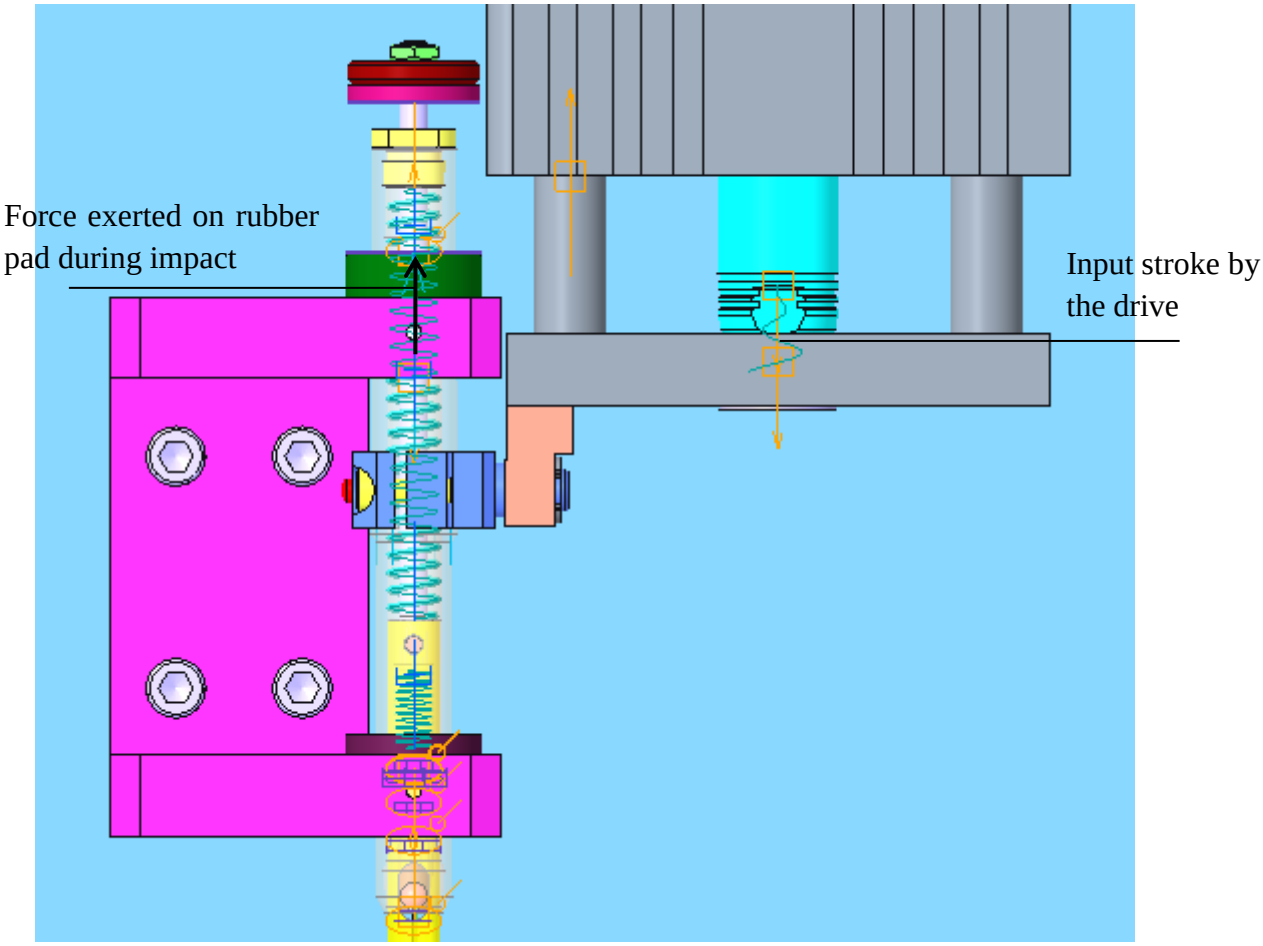

Figure 4.4: Simulation set up for new functional model

4.3. Analysis result from new needle bar mechanism

The simulation results from the analysis were taken from the control part of the needle bar during mechanical stimulation in the CREO PARAMETRIC 4.0 mechanism tool. During analysis, the needle bar behaviour was absolved for an input stroke, by creating a measuring point on the top of the needle bar control unit. The dynamic analysis results for various kinematic parameters like Position, Velocity, and Acceleration were taken and compared with input stroke using an MS excel sheet shown in graphs 4.4 to 4.6. This analysis describes

the behaviour of the original mechanical system of the needle bar with a linear servomotor, which will be further compared with the behaviour of the modified needle bar of the mechanical system.

Graph 4.4 shows the position comparison between the input stroke function from the drive and the output response measured on the control part of the needle bar. The blue curve represents the position of the needle bar shell which indicates a real stroke of 32mm and the red curve describes the position of the needle bar control unit which is the response curve for the given stroke.

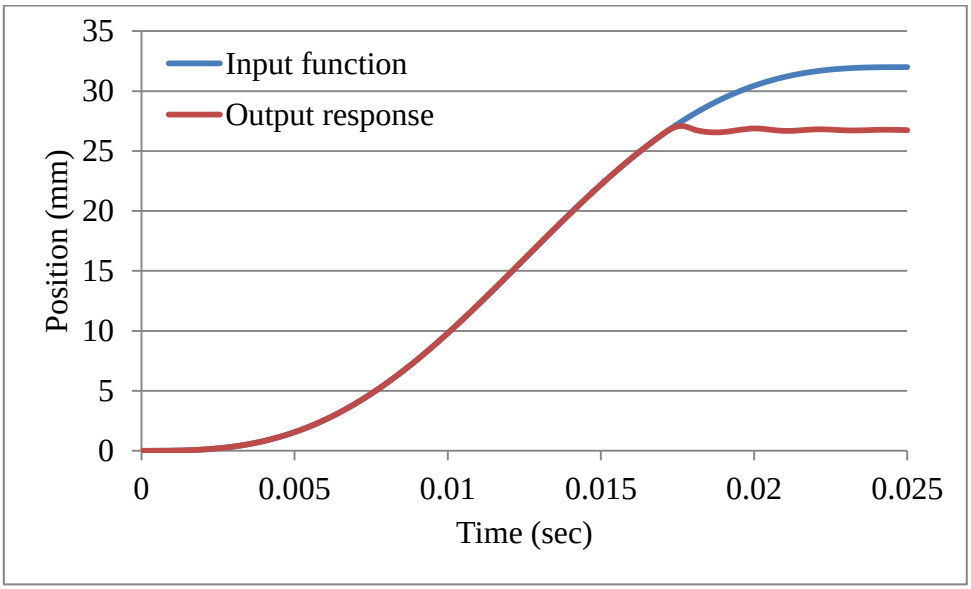

Graph 4.4: Position curves comparisons between input stroke and output response

Graph 4.5 shows the velocity comparison between the input stroke function in the blue curve by the drive and the output response in the red curve measured on the control part of the needle bar. Vibration at the time of impact of the control part on the needle bar machine frame is visible from the graph. So this thesis work aims to make a design modification of the control part of a needle bar to reduce the vibration. Further chapters will describe the modification of the control part.

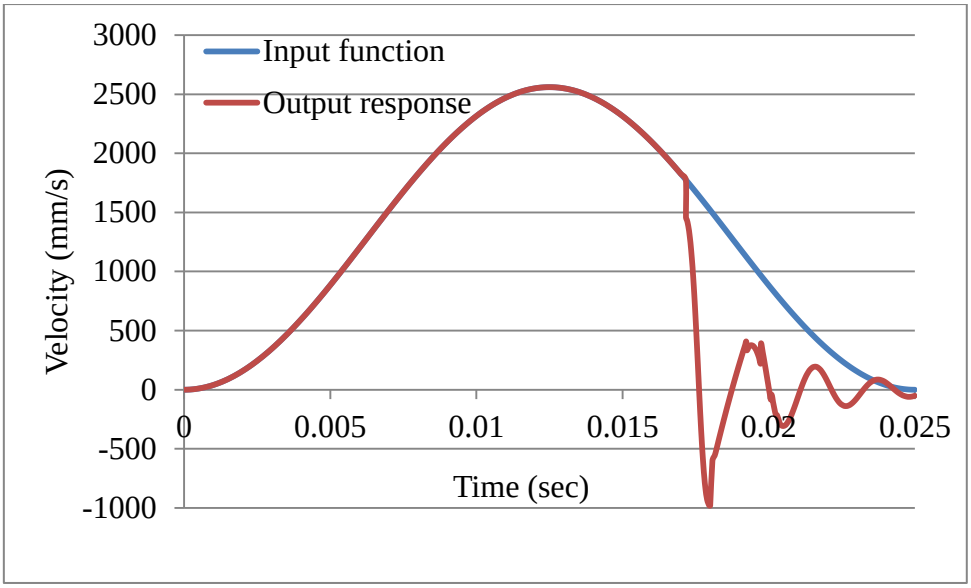

Graph 4.5: Velocity curves comparisons between input stroke and output response

Graph 4.6 shows the acceleration comparison between the input stroke function (blue curve) from the drive and output response (red curve) measured on the control part of the needle bar.

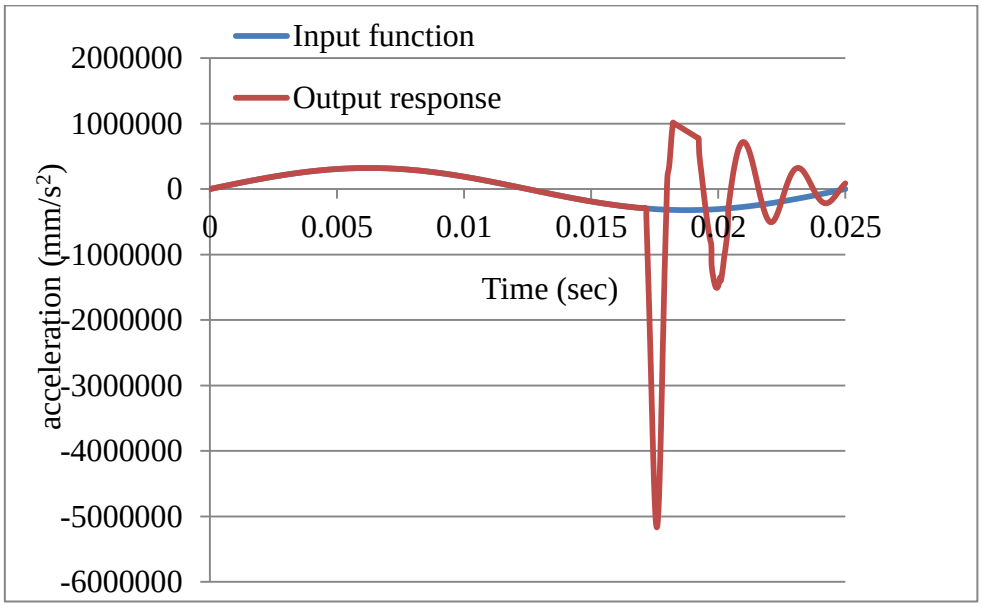

Graph 4.6: Acceleration curves comparisons between inputs stoke and output response

The mathematical model with the dynamic behaviour of the mechanical system of the needle bar described above is without the influence of the cam and gear mechanism. From the result of the analysis, it is clear that vibrations are excited due to the impact of the control part **[13]**. Furthermore, these results were used to compare the behaviour of the modified needle bar system.

CHAPTER 5. Proposal for modification to the needle bar

The analysis result of a newly modified functional model with linear servomotor shows the other reason for noise and vibration in the functional model is the impact of the control part rubber pad on the needle bar machine frame. Because of this impact, the loss of kinetic energy makes the model to generate a high level of noise and vibration while working. It is necessary to ensure that vibrational loss can be reduced without affecting any productivity in the system. By making use of the TRIZ tool, it is possible for finding parameters to control in the needle bar. The below section describes TRIZ, and the way used to find the optimization in the model parameter.

5.1. TRIZ method to find optimization

TRIZ is a problem-solving tool, used in many engineering problems to find out the solution. TRIZ can be abbreviated as “The Theory of Inventive Problem Solving”, which can be defined as a systematic approach for understanding and solving a problem through clear thinking and innovative ideas to generate a suitable solution to an existing problem **[14]**. Thanks to “TRIZ 40 by solid creativity” TRIZ software for helping to find the parameters that need to be modified in the needle bar to reduce vibration and noise on the existing system **[15]**.

According to this software to reduce vibration and noise by keeping speed and productivity constant, it can be modified by changing the state from static to movable. This can be achieved by making stationary elements to the desirable movement during impact, which means converting a part of potential energy into kinetic energy of the whole system or selected problem existing part. It will cause difficulty in transferring the needle from the upper needle bar to the lower needle bar, since the stationary part is necessary to do that, as like the machine frame in the existing functional model. This can be achieved by using some cushioning machine frame that makes prolong the impact time and simultaneously reduces the impact force.

Also, the use of gas and liquid parts of an object instead of solid parts like filled with liquids for an empty area, air cushion, hydrostatic, hydro-reactive methods. This will be a good idea of transferring solid material to the fluid to reduce the loss of vibrational energy. In the existing mechanism, it is also possible to use a fluid damper like a pneumatic damper, or Hydraulic damper along with a solid mechanical damper.

Also by changing the degree of flexibility by an adjustable damping order, reduces the noise in a control part. Use of vulcanize rubber to change its flexibility and durability, which is already existed in the model. As mentioned in the above statement, in the place of a solid damper it is possible to use fluid dampers with a high degree of flexibility to reduce the vibration and the noise in the exiting control part by prolonging its impact time.

Last but not least, by using field activated partials like ferromagnetic material. Heat a substance containing ferromagnetic material by using a varying magnetic field. When the temperature exceeds the Curie point, the material becomes paramagnetic and no longer absorbs heat. So while using ferromagnetic material, care should be about the operating temperature of the system. But the existing model will not exceed the Curie point, so it can be used irrespective of its operating temperature.

5.2. Cause and remedies for vibration in a system

One or more factors can cause vibration at any given time, the most common being imbalance, misalignment, wear, and looseness. Imbalance can be caused by a heavy spot in a rotating component. Vibration can be created when the unbalanced weight rotates around the machine's axis, creating a centrifugal force. Misalignment is also a vibrational source mainly found in the coupling point. There may be a small misalignment between motor and connecting part can also have a chance of creating a vibration in a system. Wear may be caused by impact or unnecessary mating between two parts; it is one of the main reasons for vibration in the existing functional model of the needle bar.

The necessary step to reducing vibration is by making sure that the machine is placed on a flat and balanced surface. It is a good idea to use a rubber mat to absorb vibration and stabilize the machine that saves the sewing table and reduces the wear between machine parts by stabilising its motion. Other ways to reduce vibration are listed below;

Moreover, the primary way to reduce vibration and noise in the system is by reducing the kinetic energy. Kinetic energy is the production of energy by an object in motion. There are three subcategories of kinetic energy, including vibrational which is caused by objects vibrating; rotational which is caused by moving objects; and translational which is caused by objects hitting one another in a straight path.

$$E_k = \frac{1}{2}mv^2 \qquad 5.1$$

According to equation 5.1, it is necessary to decrease the mass (m) of a moving part or the operating speed (v) of a moving part to reduce the kinetic energy (E_k). As mentioned before to reduce vibration it is necessary to reduce the kinetic energy of the control part of the exiting model. It is more effective to reduce velocity than the mass because of its power without reducing the system operation speed since it will affect productivity. It is also possible to reduce the mass of the system to reduce overall kinetic energy.

Temperature affects the kinetic energy in gas the most, followed by a comparable liquid, and then in a comparable solid. So it is best to work at a lower temperature to reduce the kinetic energy of the control part, simultaneously helps to reduce vibration in the model

Charles' Law: (Temperature-Volume Law) this law states that the volume of a given amount of gas held at constant pressure is directly proportional to the kelvin temperature. As the volume goes up, the temperature also goes up, and vice-versa **[16]**.

If the atoms are closely packed or densely packed they will have high binding energy, but less kinetic energy as in most of the solids. If atoms are loosely packed such as in fluids the binding energy and the kinetic energy are in a moderate value. This principle applies to the stationary part; during impact, solid will exhibits less kinetic energy when compared to fluids. So is better to use highly dense material for the support frame and a machine frame.

$$P = mv \tag{5.2}$$

$$F = \frac{dp}{dt} = \frac{d(m.v)}{dt} = m.\frac{d(v)}{dt} = ma \tag{5.3}$$

Another way to reduce impact force is by reducing the momentum (p) which will be the product of the mass (m) and the speed (v) shown in equation 5.2. So the reduction of high vibrational force (F) existing on the control part can also be done by increasing the time of impact along with reducing the mass and speed on the control part. Above equation 5.3 shows it is possible to reduce force by reducing mass, velocity, or acceleration of the control part also by increasing impact time.

5.3. Proposal used to reduce vibration in the needle bar of the mechanical system

It is necessary to reduce the vibration and noise generated from the impact of the rubber pad of the control part with the machine frame. So it can be modified in the design of the

existing needle bar or make use of a new component for modification. The below section explains the proposal for modification of the needle bar for an existing functional model with a linear servo motor.

5.3.1. Modification by using magnets

It is possible to reduce sudden impact by using two permanent magnets by placing like repulsive side facing each other. By attaching one magnet on the moving control part other on the stationary machine frame; it is possible to reduce sudden collision between the rubber pad and the machine frame because the repulsive force between the magnets always tried to keep them apart. Again it is possible to use electromagnet for this proposal. It is also possible to use electromagnets in two variants, by placing one electrical controlled magnet and another permanent magnet or by using both electromagnets. By placing a single electromagnet on the machine frame is an advantage of reducing inertial force and by placing a permanent magnet on the moving control part. When both the magnet is about to collide, the electromagnet gets activated and causes the magnet to repulse each other, which helps to reduce sudden impact subsequently reduce the vibrational problem.

The Neodymium magnets (NdFeB) are the most widely used permanent magnet made up of an alloy of Neodymium, Iron, and Boron. Figure 5.1 shows the sketch diagram of the design proposal. Selected permanent magnets placed one on the control part and another on the machine frame. Chapter 7 explains the selection of magnet, dynamic analysis using a modified needle bar also the comparison between kinematics parameters by dynamic analysis results between the functional models without any modification and with modification using magnets

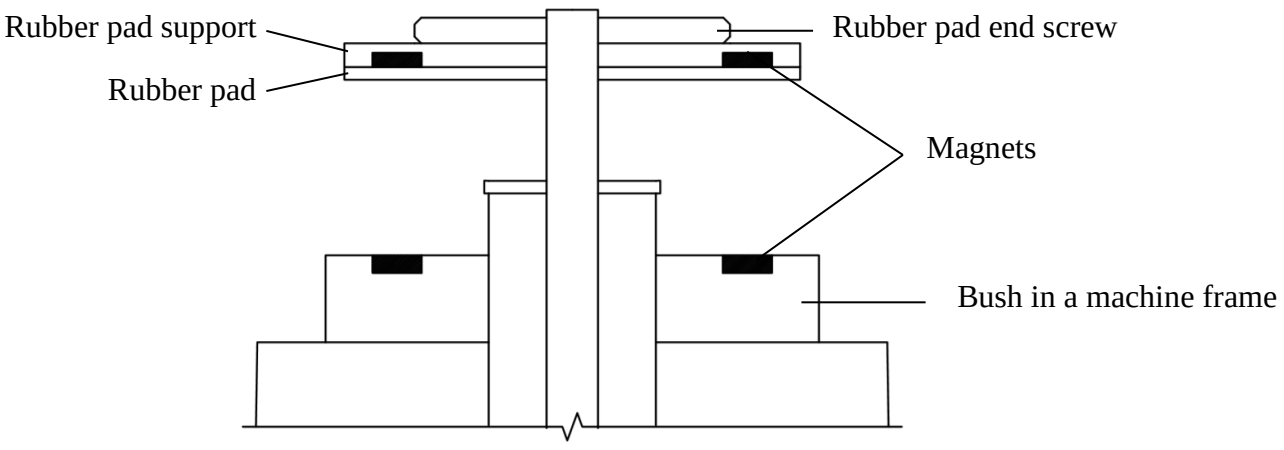

Figure 5.1: Modification of needle bar using magnets

5.3.2. Modification by using an isolator

An isolator is a tool used to reduce vibration. It had many variants but for an existing problem on the needle bar compact wire rope isolator (CWRI) and High energy rope mount (HERM) will be the best because of their compactness. The functionality of the wire rope isolator and high-energy rope mount is the same but having a slight structural difference. Below figures 5.2 and 5.3 shows the outlook of WRI and HERM.

Figure 5.2: Compact wire rope isolator [25]

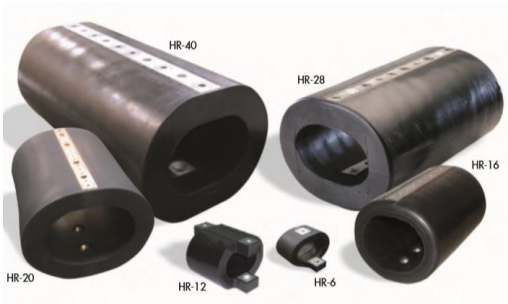

Figure 5.3: High energy rope mounts [25]

Structurally, both CWRI and HERM have two aluminium plates and the wire ropes made from steel attached between the plates. The threaded plate of WRI replaced the existing rubber pad support in the needle bar and the through-hole plate of WRI was placed simply on the rubber pad. During impact, the rubber pad will move upwards along with through holed plates with suitable design modification on the shaft. Figure 5.4 shows the two-dimensional sketch for the proposed modified model with a wire rope isolator.

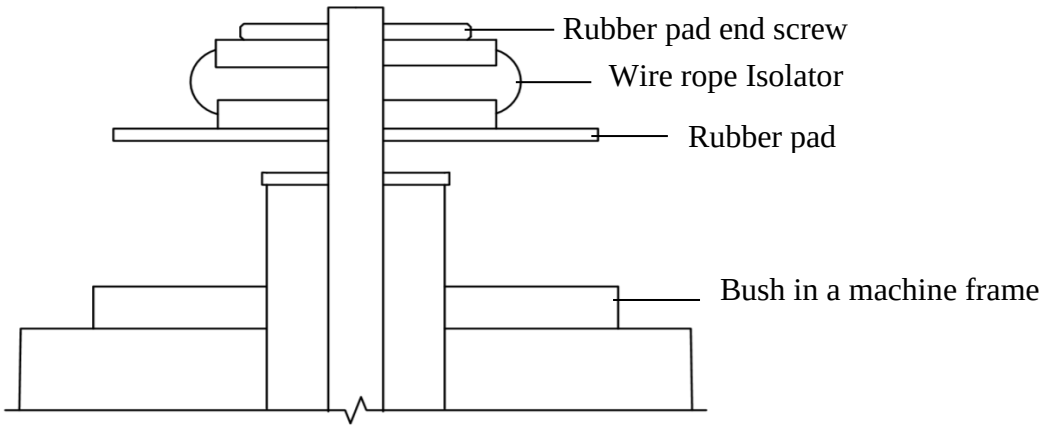

Figure 5.4: Modification of needle bar using wire rope isolator

5.3.3. Modification by using a damper

This modification can make an adaptive optimisation in the vibration, just by adding a new damper between the control part and the machine frame or by replacing the mechanical damper with a fluid damper. It also had a disadvantage in selecting a damper because of the unavailability of the required size in the market. But this principle can be used by filling a needle bar with a fluid that causes a considerable reduction in vibration because of its fluid cushioning. Various types of the damper can find applicable in the existing system, they are pneumatic damper with air as a working media and the Hydraulic damper with a liquid as working media. Another special type of damper that can find its application here is the Magneto-rheological damper (MR Damper), which works similar to an electromagnet. To activate the damper, it is necessary to pass electricity.

5.3.4. Modification by using shock-absorbing metal

It is also possible to replace the existing material with shock-absorbing material in the system. But it can able to reduce only shock but not complete vibration from the system. So it will be better to use shock-absorbing material along with another stated modification to make a considerable reduction in shock as well as vibration from the existing mechanical system of the needle bar. Sorbothane is considered super-soft polyurethane that can able to absorb shock and vibration simultaneously. Another example of shock-absorbing behaviour metal is Hardened and tempered precision strip steel **[17]**.

5.3.5. Modification in the design of the existing needle bar

Reducing the impact velocity of the control part will help to reduce the kinetic energy rapidly than just by reducing a mass (equation 5.1). It is possible to reduce the impact velocity of the control part by increasing the spring's stiffness. But the stiffness value depends on stroke, so needs to change for other stroke values. Also, it is possible to reduce the impact velocity by moving the impact position. It can be done by reducing the distance between the needle guide and ball support gripper also simultaneously increasing the distance between the rubber pad and machine frame. Even a combination of higher stiffness value and changing of the impact position will help to reduce the impact velocity better **[18]**.

Reduction of the braking force of the control element can be done again by reducing the mass and speed of the control element, and by increasing the impact time (equation 5.3). It can be done by using a flexible or cushioning block bush in the machine frame also with a geometric modification by conical bush and tapered rubber pad **[19]**.

5.4. Used modification from the above proposal

In this thesis work, modification of the functional model with a linear servomotor was done to perform modification on the needle bar. For better analysis and by taking advantage of the symmetry of the functional model, the model was changed. The new functional model is only half of the original model. That means a new modified functional model with only an upper needle bar with its linear servomotor connection.

Regarding modification on the needle bar, both vibration isolation and vibration absorber methods are used. In this thesis work, a compact wire rope isolator (CWRI) was used as a vibration isolator and a permanent magnet as a vibration absorber called Magnetic Vibration Absorber (MVA) as a modification proposal to conduct dynamic analysis. Chapter 6 will describe the modification of the needle bar with a compact wire rope isolator and at the end of the chapter; the results are compared with the original model without any modification. Also, chapter 7 will describe needle bar modification with permanent magnets, and results are explained and compared with the result of the functional model without any modification.

CHAPTER 6. Modification with wire rope isolator

Wire rope isolator is a kind of passive-type vibration isolator having both springs stiffness coefficient (*K*) and a damping coefficient (*C*) with a mass element as shown in figure 6.1**[20]**. Wire rope isolator is widely used as vibration isolator and shock absorber in many industrial applications and the dynamic behaviour of wire rope isolator shows its non-linear stiffness and damping characteristics **[21][22]**.

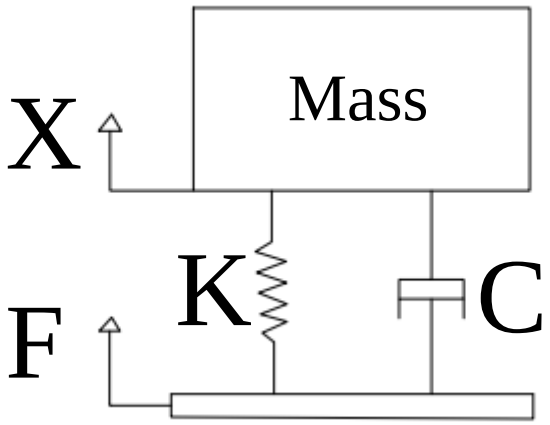

Figure 6.1: Passive isolation system [20]

Standard Wire Rope Isolators are comprised of series of stainless steel stranded cable twisted with cantered core cable arranged in leaf or helical fashion with an excellent energy dissipation capability due to friction between wire cable during loading and unloading which exhibits friction damping (coulomb damping) between the cables in an isolator **[23][24]**. Steel cables are threaded through two Aluminium alloyed retaining bars that are mounted for effective shock and vibration isolation. Wire rope isolator having various advantages like corrosion resistance, great adaptability, excellent reliability with a higher lifespan, can operate in the wide temperature range (-180º to +300º), and anti-vibrational and shock mounts in multi-direction.

Wire rope isolator [WRI] is of various kinds like Compact wire rope isolator [CWRI], Helical wire rope isolator [HWRI], Polycal wire rope isolator [PWRI], High energy rope mounts [HERM], etc. Because of the compactness and great adaptability of CWRI, it was taken as a modification tool for modifying the needle bar. The used CWRI is of the series GGD1.6-11.2/17.8/4L/MB having a width of 17.8 mm and height of 11.2 mm which is a pre-existing standard offered by the company ENIDINE **[25]**.

6.1. Design modification of the functional model

Design modification for the functional model with selected compact wire rope isolator was done with the help of the CREO PARAMETRIC 4.0 modelling tool. Later dynamic analysis was done to compare the kinematic behaviour of the modified functional model. Figure 6.2 shows the modified functional model with a compact wire rope isolator.

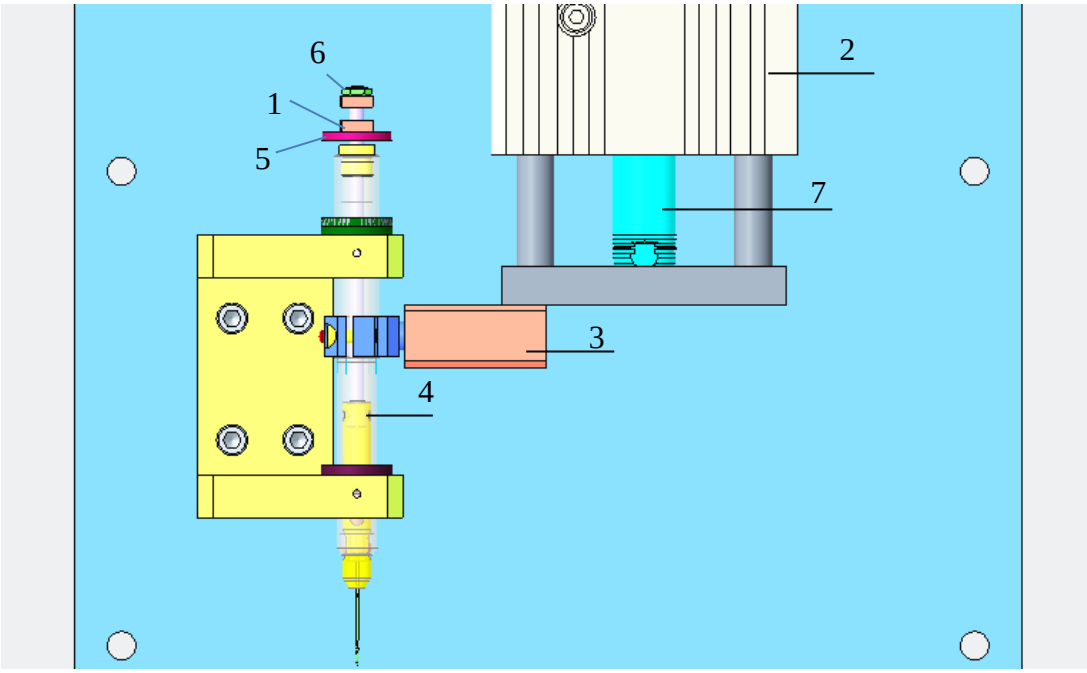

Figure 6.2: Detailed view of the modified functional model with WRI

The new functional model was designed by a Compact wire rope isolator 1 which is attached to the control part of the needle bar. With a single linear servomotor 2, the model design became easy and simple compared to the design with two servo motors used earlier. The new connecting part 3 that connects between the servomotor and the needle bar 4, helps to transfer the linear motion from the spindle 7 of the motor to the needle bar shell. The whole setup was placed on the supporting plate, supported by the rigid supporting frame.

The modified component compact wire rope isolator 1 is attached between the rubber pad 5 and rubber pad end screw 6. The design clearly said a compact wire rope isolator plate replaces the rubber pad support in the control part. The used compact wire isolator is having threads on one plate end and the other plate end is having a through-hole. The threaded side isolator is connected with a screw end in the top of the needle bar rigidly and the through-hole will be placed above the rubber pad that can access motion. Design modification was done to keep the rubber pad and isolator's endplate together, shown in figure 6.2.

Working of the newly modified model is similar to the earlier unmodified functional model. The input movement can be given by linear servomotor by the suitable stoke function. With the help of the connecting part, the movement gets transferred to the needle bar so now the needle bar will move in linear reciprocating movement. During the impact of the rubber pad with the machine frame the isolator will get compress at its maximum displacement then the release of a needle from the needle bar will be taking place as earlier. The wire rope isolator will be acting as an energy storing device here in which the impact force from the frame will be stored in it and release while traveling in its second phase. The reason to keep the rubber pad in the model is to avoid the sudden impact of the frame with the isolator, further; it will prevent the compact wire rope isolator and prolong its functional period.

6.2. Analysis for the modified functional model

Dynamic analysis for the selected compact wire rope isolator was done for a modified functional model with the CREO PARAMETRIC 4.0 mechanism simulation tool. Figure 6.3 shows the simulation setup for the functional model with the compact wire rope isolator along with its force definition.

The modified functional model with CWRI on the needle bar makes used a simple Cycloidal displacement (sinus acceleration) function with an operating speed of 250 RPM and the working stroke of the needle bar is 32mm. The mathematical model is extended by parameters describing the wire rope isolator, like force (stiffness) and damping. Figure 6.3 shows the modified functional model with CWRI with a force in the direction exactly opposite to the direction of the applied movement. CWRI act as a spring with a non-linear stiffness or varying force-displacement characteristics. The characteristics graph for the chosen compact wire rope isolator is shown in graph 6.1 with the parameter of force in the vertical direction and the displacement of the isolator base in the horizontal direction.

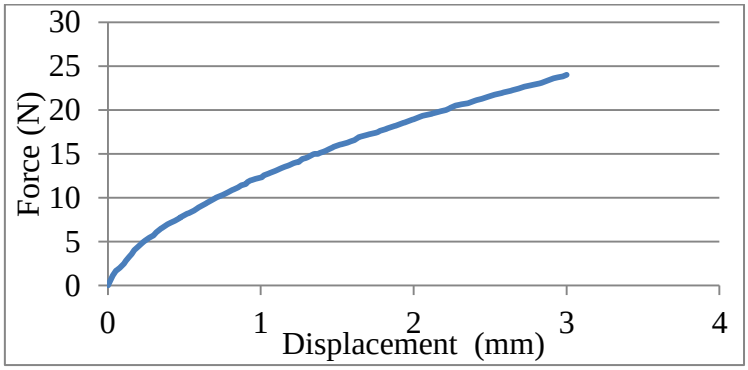

Graph 6.1: Characteristics curve for a selected wire rope isolator [25]

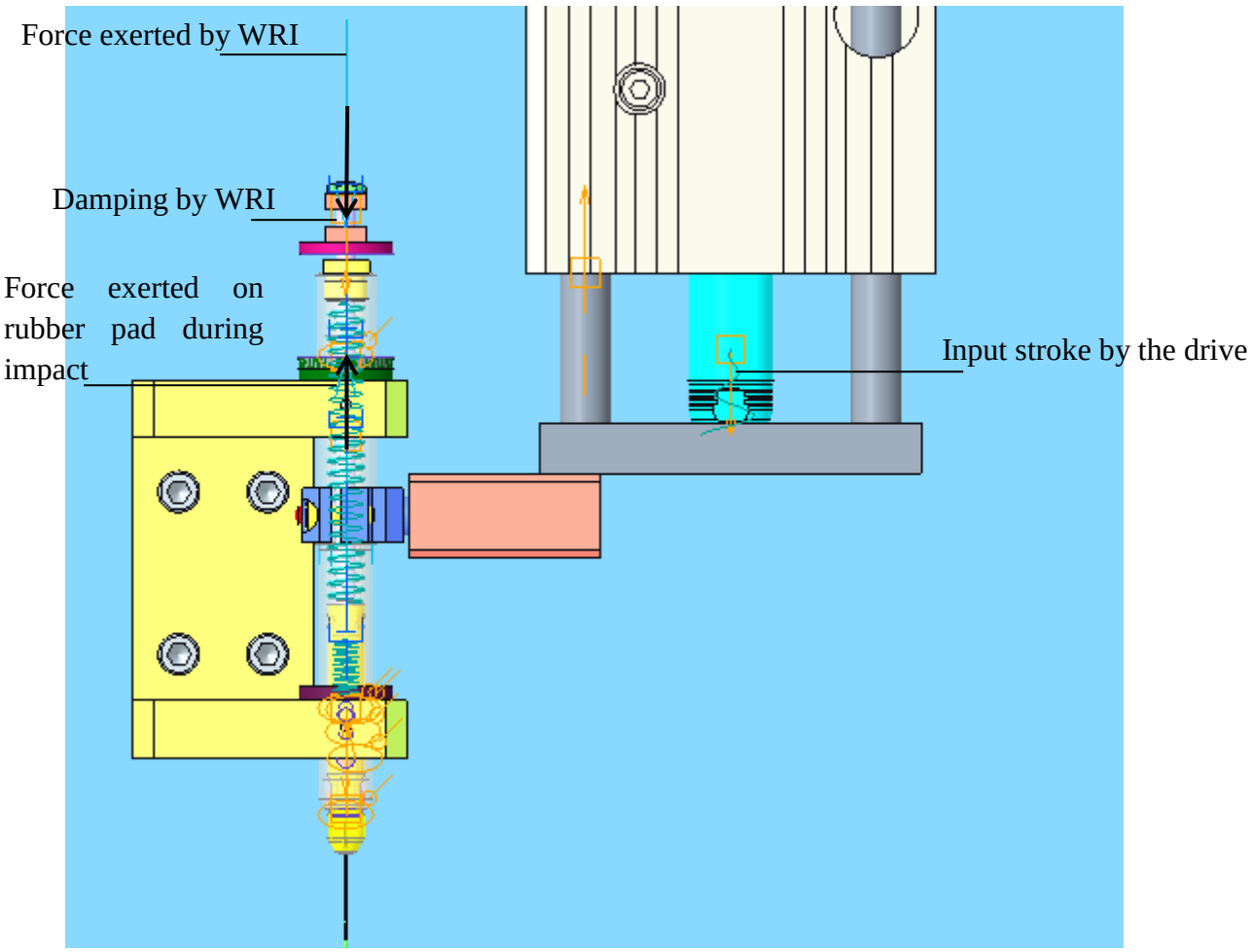

Figure 6.3: Simulation set up for modified functional model with WRI

As in kinematics to reduce the vibration in the system, it is necessary to exhibits damping. As with stiffness, damping is also having non-linear behaviour for compact wire rope isolator, but it is impossible to add nonlinear damping value to the functional model due to software limitations. So the work is limited to constant damping value. The damping calculation for the selected isolator was done by using the fundamental critical damping equation. But this value is not precise, so based on the theoretical basis of dynamic mechanism and the damping by rubber pad in the model along with the critical damping calculation result of the damping value for compact wire rope isolator was estimated as $0.03 N.sec.mm^{-1}$(see appendix 5 for calculation part). Later damping value was inserted into the functional model and dynamic analysis was performed.

The analysis results are obtained from the model during mechanical simulation using the CREO PARAMETRIC 4.0 simulation tool. During analysis, the needle bar's behaviour was observed for an input stroke function to the drive. By creating a measuring point on the top of the needle bar's control unit, the behaviour of the newly designed modified functional model

was observed. The dynamic analysis results for various kinematic magnitudes (position, velocity, acceleration) are showed in graphs 6.2 to 6.4. The results are compared with the input stroke function.

Below graph 6.2 shows the position comparison between input function and the output response of the modified functional model with compact wire rope isolator, the blue curve shows the input stroke taken from the needle bar shell. As mentioned, the working stroke of the functional model is 32mm is shown in the y-axis. And the working period of the complete sewing cycle is 360º (2π), but the motion followed by the upper needle bar to transfer needle from upper needle bar to lower needle bar is 60º corresponding to a time of 0.025sec it is mentioned on the x-axis of the curve. The output curve will also follow the same curve as like input but after the impact curve changes because it was taken from the control part, shown in the green curve.

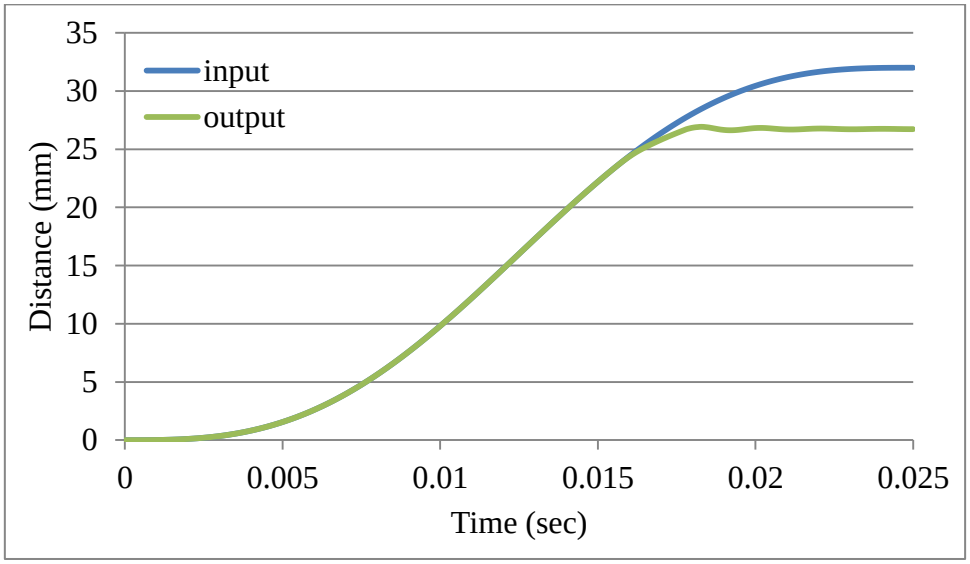

Graph 6.2: Position comparison between input stroke and output response for a modified model with WRI

Graph 6.3 shows the velocity comparison between input strokes from the drive to output response curve for a modified functional model with a compact wire rope isolator. The blue curve represents the input stroke which was set by the Cycloidal (sinus) stroke function for an operating speed of 250RPM. The green curve is the response curve obtained from the control part of the needle bar. Curve shows after 0.018sec having vibration oscillation curve this is because of the impact between the machine frame and rubber pad. Compact wire rope isolator is having better damping characteristics to avoid loss by the kinetic energy. At the

end of this chapter, the value of the reduced energy is mentioned and it is compared with the original functional model without any modification.

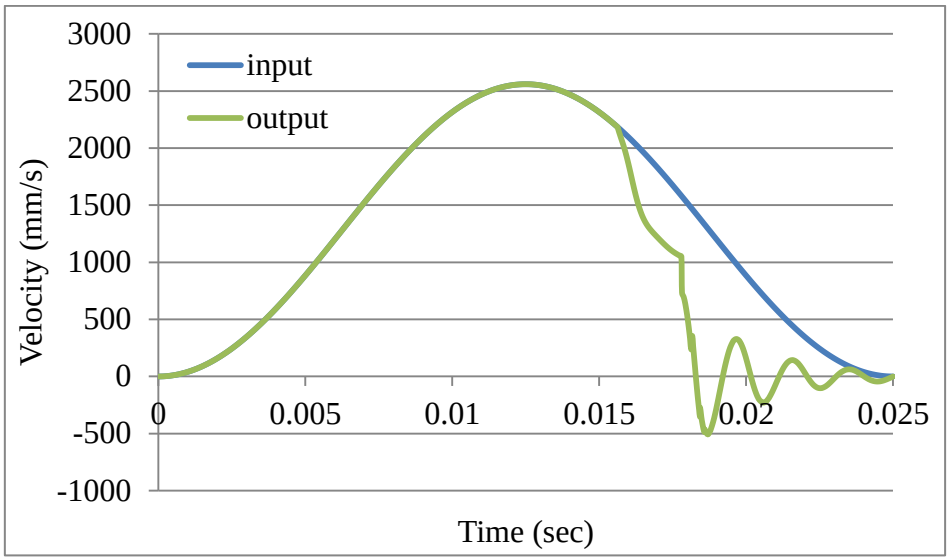

Graph 6.3: Velocity comparison between input stroke and output response for a modified model with WRI

Furthermore, graph 6.4 shows the acceleration comparison between input stroke from the drive and output response curve for a modified functional model with a compact wire rope isolator. The blue curve represents the input stroke by Cycloidal (sinus) stroke function for an operating speed of 250RPM. The green curve is the response curve obtained from the model on the control part of the needle bar. It was just a derivative of the above velocity curve.

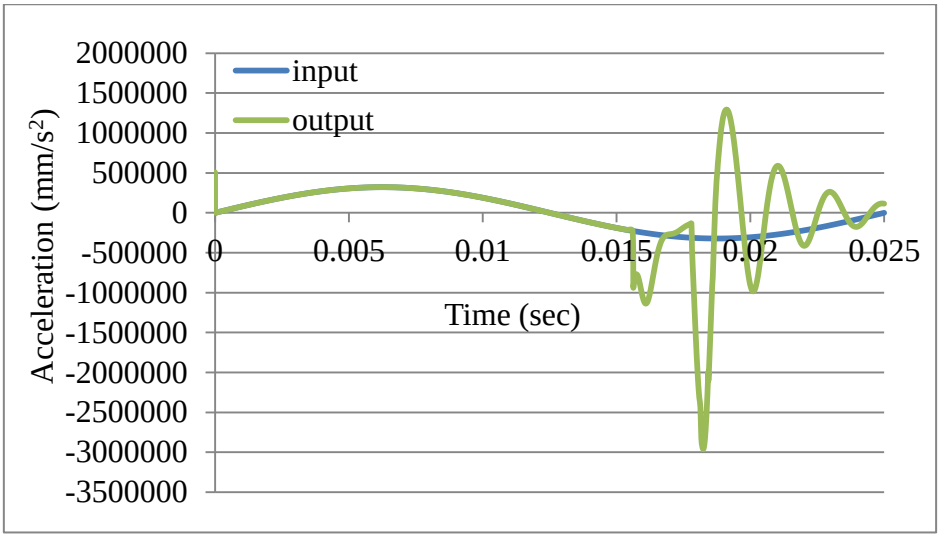

Graph 6.4: Acceleration comparison between input stroke and output response for a modified model with WRI

6.3. Result comparisons

The results obtained from the CREO simulation were transported to an excel sheet to compare the results between input stroke with the output response from an original model without any modification below graphs 6.5 to 6.7 show the comparisons between different kinematic parameters.

Graph 6.5 shows the Position comparison between input stroke (blue curve) and output response of the modified functional model with a compact wire rope isolator (green curve) also with the functional model without any modification (red curve). From the curve, it has shown that the response of the functional model with modification follows the proper way as a functional model without any modification which is necessary for the functionality of the needle transfer mechanism.

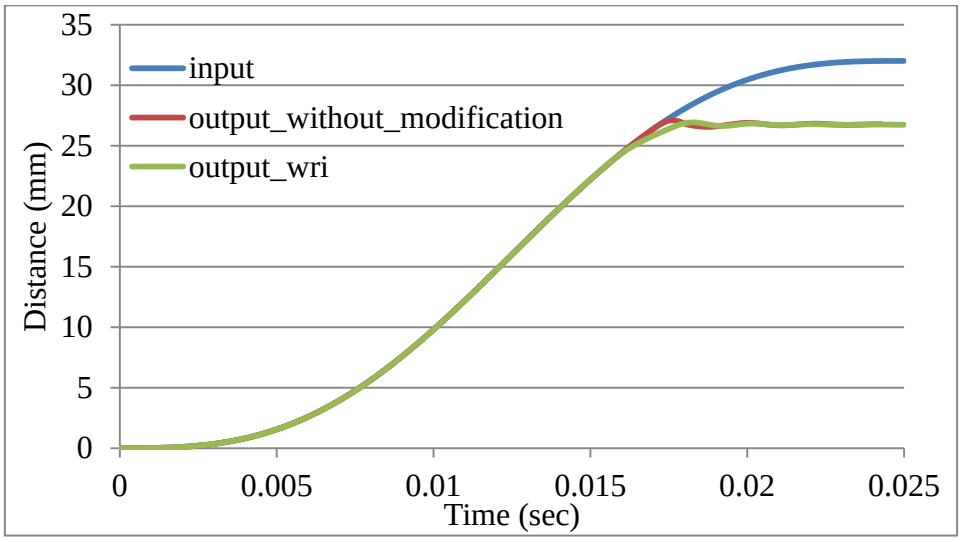

Graph 6.5: Position comparison between input stroke, the output response of the modified model with WRI and with the original unmodified model

The very important parameter to compare the loss of kinetic energy from the model is velocity. Graph 6.6 shows the velocity comparison between all three curves, input drive and output response from the functional model with wire rope isolator and without any modification to the control part. As explained before there is a vibrational oscillation after the impact of the control part on the rigid frame. In the graph red curve represent the response curve from the model without any modification had bigger amplitude in velocity when compared to the green curve; represents the response curve from the control part of the model with a wire rope isolator modification. The curve gets a better look with a reduced velocity oscillation because of self-damping by the wire rope isolator.

Sl no	Velocity of the unmodified model (m/s)	Kinetic energy of the unmodified model (J)	Velocity of the modified model (m/s)	Kinetic energy of the modified model (J)
1	0.4073861	0.01681	0.3189016	0.01024

Table 6.1: Kinetic energy comparison between the models

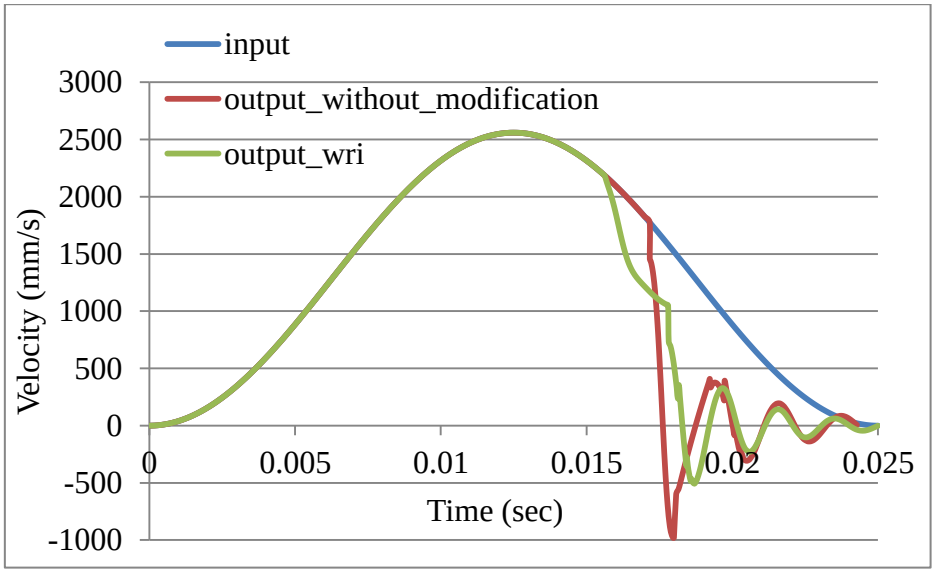

Graph 6.6: Velocity comparison between input stroke, the output response of the modified model with WRI and with the original unmodified model

The kinetic energy table 6.1 shows the velocity value at the time of impact between the rubber pad and the needle bar machine frame. With the necessary kinetic energy equation by knowing mass and velocity value at the time of impact, loss of kinetic energy was found. It is possible to reduce almost 0.0064J or 6426.52kg.mm^2.s^{-2} energy of vibration by using a compact wire rope isolator.

The acceleration comparison between input (blue curve) and both the output with the modified functional model with wire rope isolator (green curve) and the functional model without any modification (red curve) is shown in graph 6.7. As it is seen from the graph the amplitude of the acceleration is also reduced drastically as seen in the velocity curve.

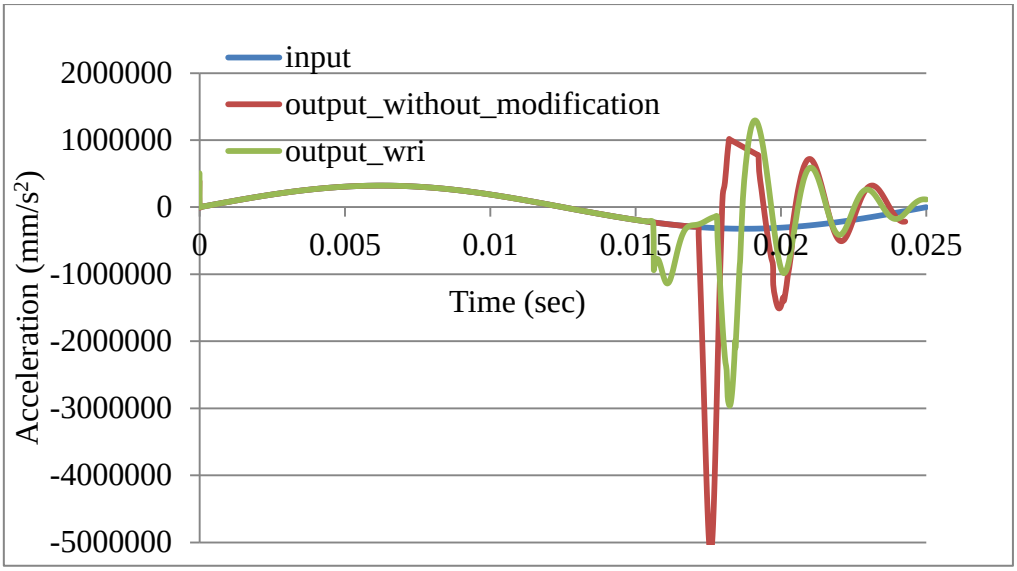

Graph 6.7: Acceleration comparison between input stroke, the output response of the modified model with WRI and with the original unmodified model

The above dynamic analysis results and comparison clearly show that it is possible to reduce the vibrational loss on the functional model with the help of a compact wire rope isolator. The next chapter explains about modification of the functional model with a permanent magnet, which was the second proposal for this thesis work.

CHAPTER 7. Modification with permanent magnets

As already mentioned in chapter 5, parameters like mass, speed, and time can be altered to reduce kinetic energy (see equations 5.1, and 5.3). Two permanent magnets of the same size or different are placed one on the control part and another on the machine frame facing like pole each other. When magnets start moving each other, repulsive force between them allows the magnets to keep away from each other. By this modification of permanent magnets on the available needle bar, it is possible to reduce impact speed by increasing the impact time can further lead to a reduction in the loss of kinetic energy from the control part due to impact.

A vibration absorber is a method used to absorb and minimizes the vibration in the system. The widespread method of vibration absorber is tuned mass damper which helps to reduce the amplitude of the vibration in many structural problems. **Sayyad et,** al proposed the way of using Magnetic Vibration Absorber (MVA) by using permanent magnets placing like poles facing each other. The repulsive force between the magnets can act as a spring constant can be treated as a restoring force that acts on the magnet to form a mass element on the absorber **[26]**. **Yao et,** al stated that the vibration can be minimized by using three variants, Control of the vibration just by applying an external force, Vibration reduction can be done by modifying the parameters in the system and by using a suitable dynamic vibration absorber (DVA) **[27]**. By using a vibration-absorbing method with two permanent magnets repulsive force, the new functional model was created using CREO software and dynamic analysis was also done for the proposed model with various selected magnets.

The modification of the magnetic vibration absorber was also proposed. According to **Benacchio et, al** new way of Magnetic Vibration Absorber (MVA) can be done by tuning the stiffness by using a fixed corrective magnet parallel to the main axis **[30]**. **Valtera et, al** show the new way of MVA by modifying magnetic shape (cone-shaped) and by using magnetic pole piece that maximizes the repulsive force that works effectively for kinetic energy accumulation on the Traversing Rod **[31]**. Also **Wang et, al** proposed a new kind of vibration isolation by new quasi zero stiffness (QZS) method which has the property of high-static and low-dynamic stiffness by using a combination of springs and magnets. And he concluded that this way of vibration isolation is best suited for low-frequency vibration isolation and it is better than a normal vibrational isolator **[32]**. The proposed Modified Magnetic Vibration Absorber (MMVA) is attached to appendix 7.

This chapter includes the work on choosing the best magnetic pair and developing the force v/s distance characteristics for the selected magnets also dynamic analysis with sensitivity analysis of the newly modified functional model using two permanent magnets.

7.1. Selection of suitable magnets

The neodymium magnet (neodymium iron boron/ NIB magnet) is used as a permanent magnet for the current work. Neodymium magnet is a permanent magnet made up of an alloy of neodymium; iron, boron to form a $Nd_2Fe_{14}B$ structure. It is one of the strongest magnets when compared to other permanent magnets available as of now (samarium cobalt magnet, Alnico) **[28], [29]**. Neodymium magnet is available in various variants starting from N24 currently up to N52. More the number after N is more powerful. The Repulsive force v/s distance comparison of a different magnet of the same size for neodymium magnet is shown in graph 7.1. For this work N35 and N52 neodymium magnet were used, since N35 magnet is widely used magnet in many applications and it is easy to buy because of its abounded size availability in a market. Because of better force characteristics, a magnet of type N52 was used for theoretical verification. The magnetic properties are inserted into the functional model in CREO under the material property section during analysis.

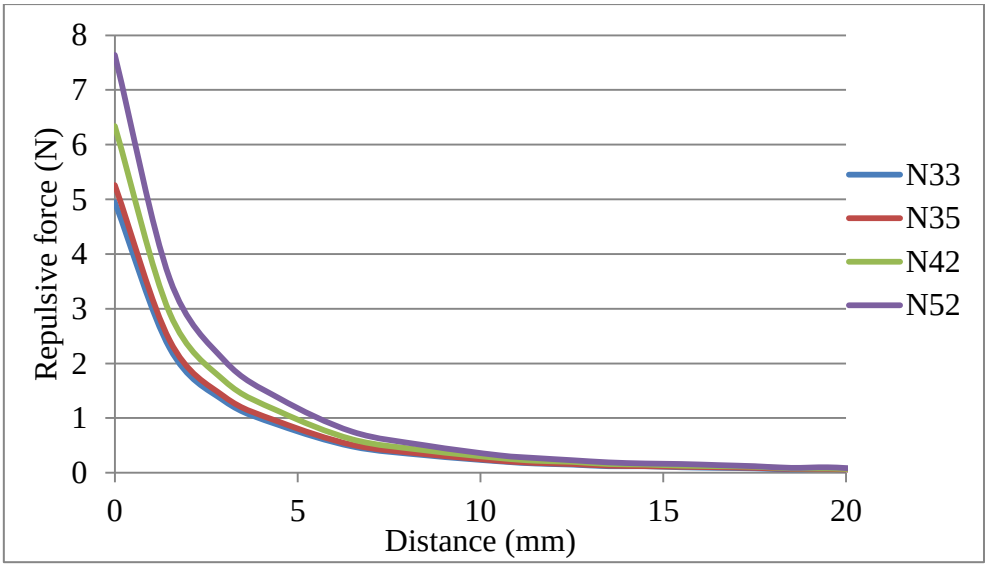

Graph 7.1: Force v/s Distance curve for different magnets of the same size

When it comes to choosing the best pair of a magnet for dynamic analysis, care should be taken in such a way that mass of control part should not be more also should have better force characteristics, in such a way that force should not be too high and nor too low for an available model. Higher forces can generate strong repulsive force between each other it will affect the needle release mechanism. Also, the lesser force will not make any changes in the

model when compared to the model without any modification. For a better comparison, two kinds of magnetic analyses were done. Firstly by increasing a height with constant width means the same inside and outside diameter of the magnet. Later by taking the best magnetic pair from this analysis and keeping its volume as a constant and changing its height and diameters. The identical magnets are used on both the control part and the machine frame for this analysis. Below figures 7.1 and 7.2 shows the two-dimensional drawing for both the variants.

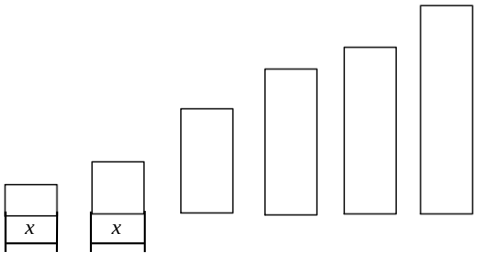

Figure 7.1: Magnets with the same width and with increasing height

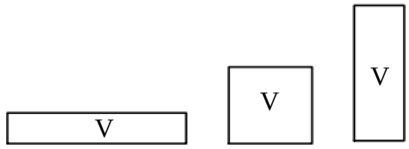

Figure 7.2: Magnets with the same volume

From the analysis result of the first variant, it is realized that by increasing the height of the magnet the repulsive force between the magnets also getting increased. See graph 7.2 for the comparison. The square magnet will be having better characteristics since the magnetic field lines are equally distributed; it is also realised from many trials and comparison between the analysis results. A square magnet is a magnet with the same width and height it is highlighted in the red curve of magnet 20_15_2.5 in graph 7.2.

In the second variant of analysis, volume was kept constant with changing other dimension parameters (width and height). Moreover, the result is shown in graph 7.3. The magnet with the square cross-section along with the other two kinds of magnet was used in this analysis and all three curves are similar but the force value of the square magnet higher than the other two magnets (see the red curve of magnet 20_15_2.5 in graph 7.3).

This analysis was done by using FEMM 4.2 software later results are extracted and compared in an MS excel sheet. The Lua script is written in appendix 3 for the selected magnetic pair. And the magnetic analysis results from FEMM 4.2 are in appendix 4.

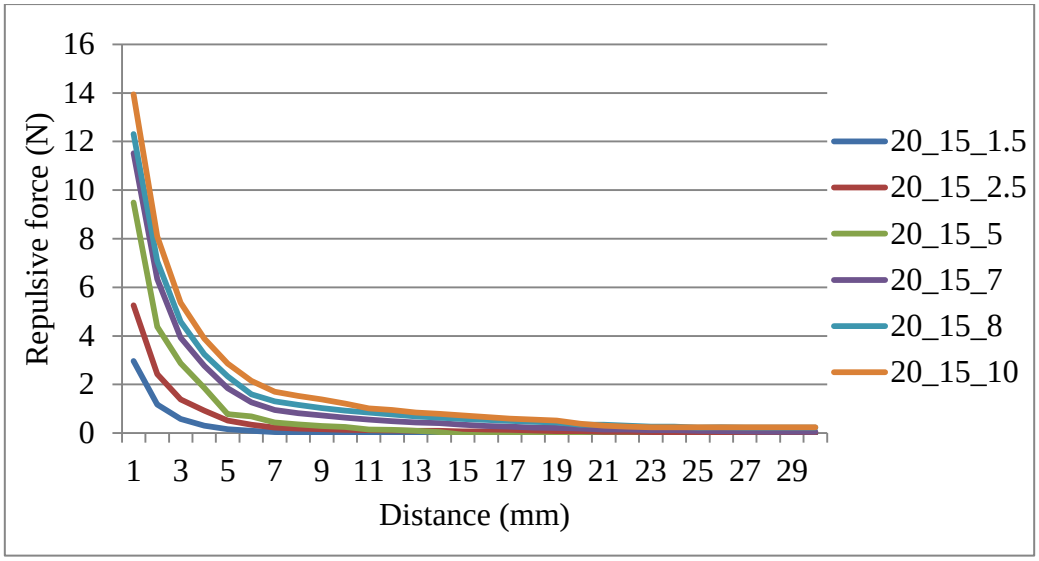

Graph 7.2: Force v/s Distance curve for magnets with the same width and by increasing height

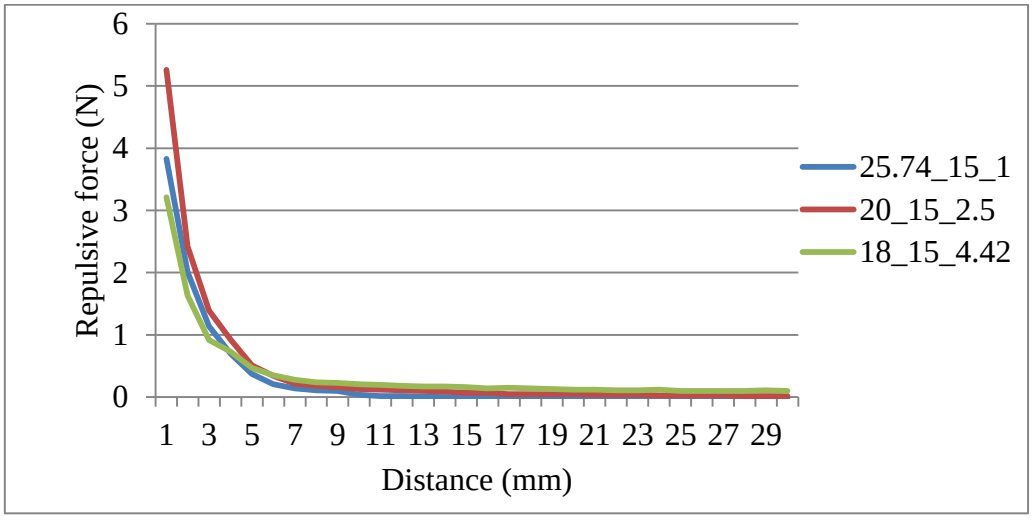

Graph 7.3: Force v/s Distance curve for magnets with the same volume

7.2. Design modification of the functional model

Design modification for the selected magnets variant was done for the available functional model with the help of the CREO PARAMETRIC 4.0 modelling tool. Below figure 7.3 shows the cross-section view of the design modification with permanent magnets.

The new modified functional model was designed by using permanent Neodymium magnets 1 as a modified component. With the help of a single linear servomotor 2 model, the design becomes easy to analyse when compared to two servomotors in a design that was done earlier. With the help of new connecting part 3 that connects between the servomotor and the needle bar 4 which helps to transfer the linear movement from the servo motor to the needle bar.

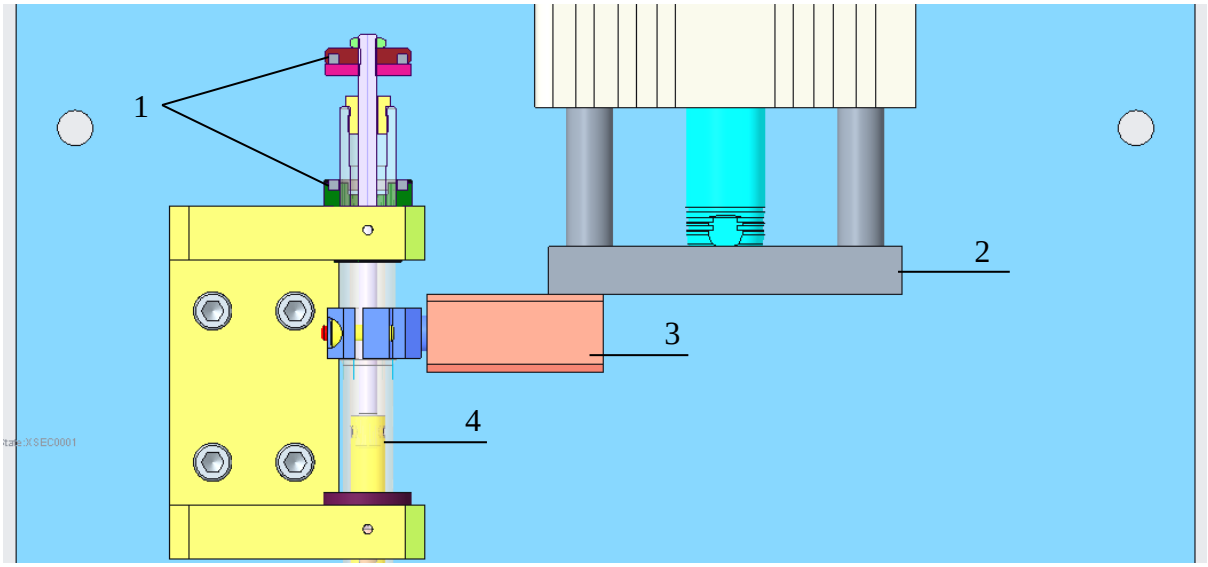

Figure 7.3: Detail view of the modified functional model with permanent magnets

As in the modification of the compact wire rope isolator here as well modification of design was done in such a way that it should get a lesser mass on the control part. So non-moving or stationary magnet was placed on a fixed needle bar machine frame and the moving magnet was kept in between the rubber pad and the lock screw of the control part. Here as well rubber pad plays an important role to prevent damage while working. Both the magnets are facing like poles towards each other. If the distance between two magnets starts decreasing the repulsive force between them will be getting increased, according to the force v/s distance curve obtained from FEMM analysis. It caused the magnet to keep away from each other and will prevent a sudden collision between the control part and the machine frame support. But as in the Wire rope isolator modification, rubber pad support was completely removed as a part of design modification but the magnet placed inside the rubber pad support with a simple design modification just by grooving with the dimension of the magnet. Figure 5.1 shows the two-dimensional drawing of the design modification of the control part with permanent magnets.

The design modification with the magnets is as simple as a design without any modification. But there will be an extra groove for magnets both on rubber pad support and block bush. The working principle of this functional model will be as same as before. The input motion is given by a linear servo motor which will be the linear movement by the desired stroke function. The motion will transfer to the needle bar from drive through connecting part 3. So the reciprocating linear motion can be exhibited by the needle bar as well. As the control part starts moving, the distance between the magnets decreases, which

mean the repulsive force between magnets getting increases, which influence the control part. For better behaviour, the force should neither be too high nor too low as well. As discussed at the beginning of this chapter so for better dynamic behaviour the magnetic pair of outer diameter 20mm, the inner diameter of 15mm with a height of the magnet as 2.5mm was selected for analysis comparison of magnet type N35. Below graph 7.4 shows the repulsive force v/s distance characteristics obtained from FEMM 4.0 analysis for the selected magnetic pair along with its cross-sectional dimension for the design.

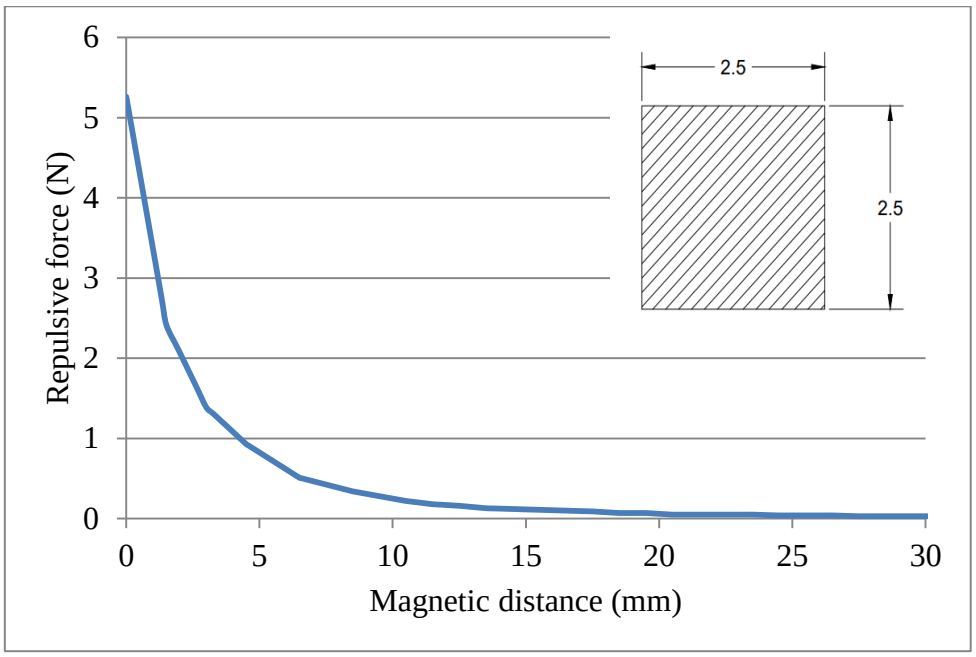

Graph 7.4: Force-distance characteristics for a selected magnet

7.3. Analysis for the modified functional model

Dynamic analysis for the selected magnet variant was done for a modified functional model with the help of the CREO PARAMETRIC 4.0 mechanism simulation tool. Figure 7.4 shows the simulation setup for the functional model with a selected pair of permanent magnets along with its force direction.

The functional model with linear servomotor makes use of the simple Cycloidal displacement (sinus acceleration) function with an operating speed of 250 RPM with the working stroke of the needle bar is 32mm. The magnet on the machine frame will create the repulsive force exactly opposite to the direction of the control part movement because the moving magnet will be on the moving control part which is against the stationary magnet. During analysis, the behaviour of the needle bar was observed from an input stroke function to the drive-by creating a measuring point on the top of the control part of the needle bar.

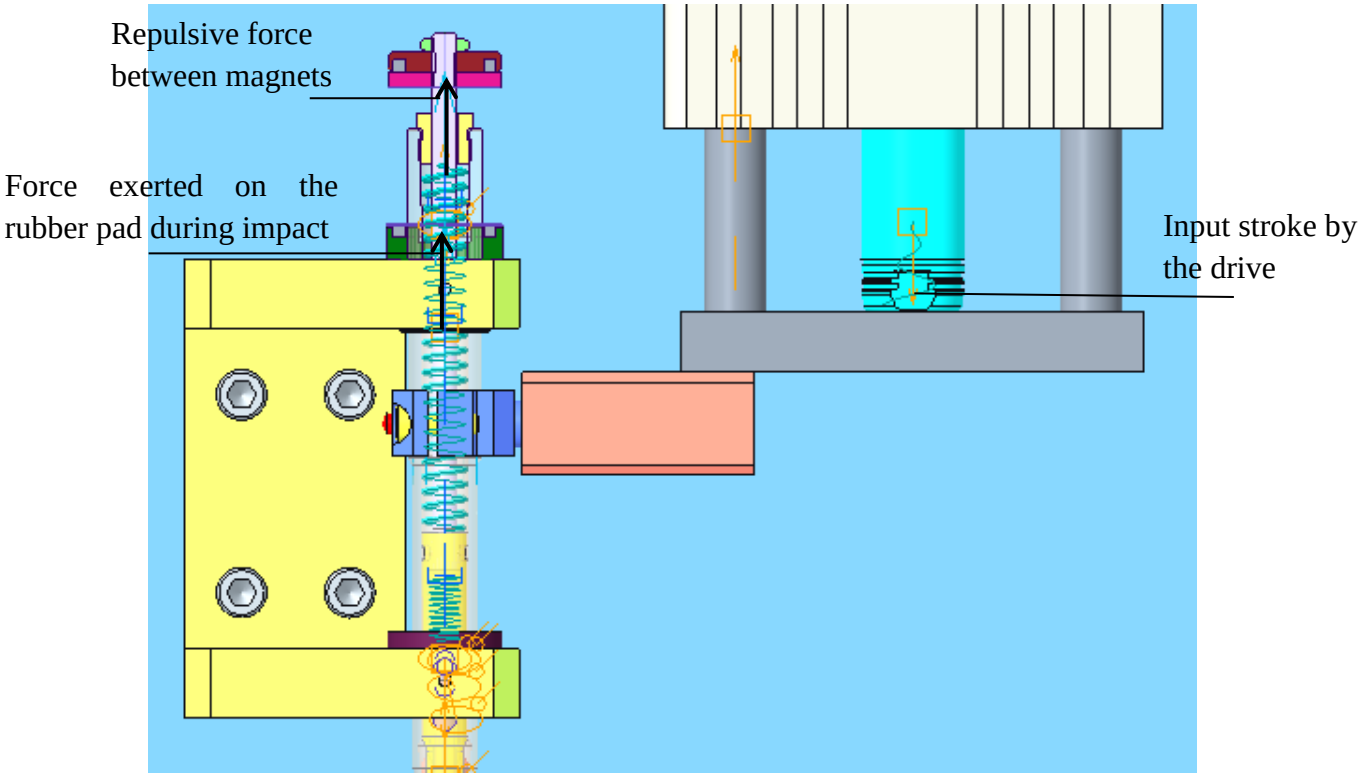

Figure 7.4: Simulation set up for modified functional model with permanent magnets

Firstly sensitivity analysis was done from the dynamic analysis result between different selected magnets of two variants of the same width and same volume which was mentioned at the beginning of this chapter. The analysis was done by choosing the maximum velocity value of the first impact during analysis and which are compared with a different value of the variant. Magnet with increasing height with the same inner and outer diameter will have increasing velocity value. Since it is a dynamic analysis there may be a chance of this behaviour just by the influence of mass without a magnetic force. So again it is necessary to cross-check the analysis result just a mass without any magnetic force. The later analysis was done by activating both mass and force. Graph 7.5 shows the sensitivity analysis for the variant with increasing height, representing the y-axis as maximum velocity after impact, and x-axis as the dimension of a magnet (same inner diameter of 15mm and the outer diameter of 20mm).

From the above sensitivity analysis, it was found that the maximum value of velocity was found at a higher magnet than at the smaller magnet for both the variants. But after reaching the desired height of the magnet, the velocity on the control part of the needle bar starts decreasing because the force influence will be bigger than the mass which was shown by the red colour curve in the graph 7.5

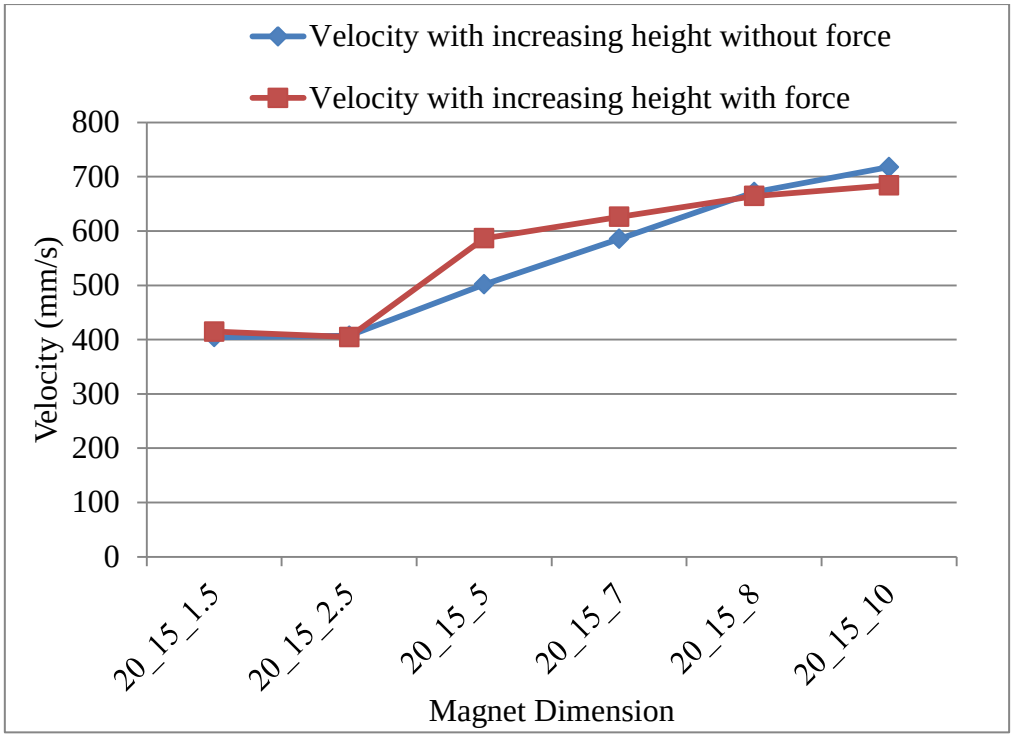

Graph 7.5: Sensitivity analysis for magnets of same base width

. By this analysis, it is clear that magnets can be used for modification to reduce vibration in the functional model. But it is necessary to do another variant analysis by keeping volume as a constant for the selected magnet. From the above sensitivity analysis of the dynamic behaviour of the modified functional model, the magnet with the same height and same width will have lesser velocity when compare with other height to width ratio magnet. A small magnet also had the same velocity value as the magnet with a square cross-sectioned magnet, square magnets had higher mass but lesser velocity because of their better force v/s distance characteristics, so that can be taken as the base for volume variant sensitivity analysis. The result of the analysis was expected that with the increasing height will have increased velocity. The comparison of sensitivity analysis of volume variant is shown in graph 7.6 for both variants with force and without force.

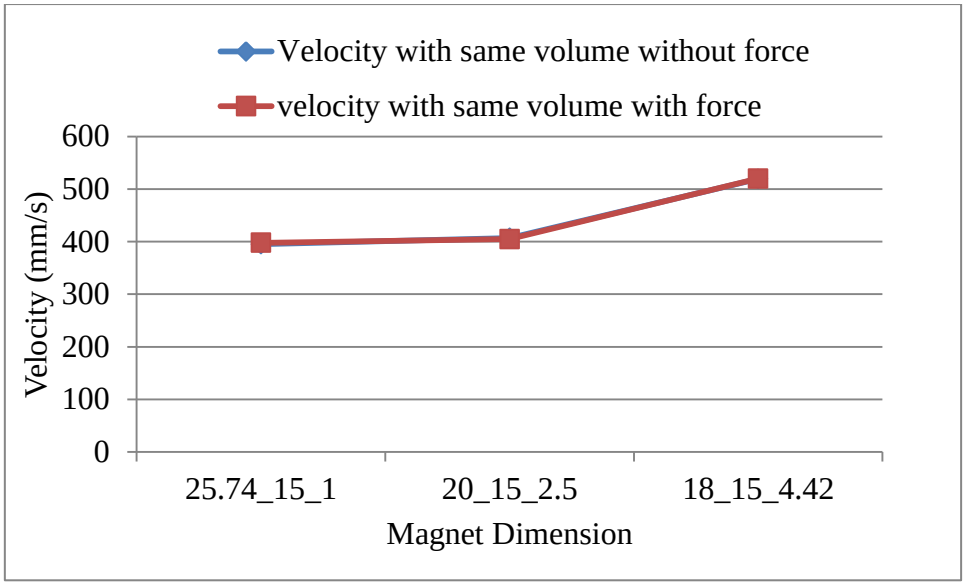

Graph 7.6: Sensitivity analysis for magnets of the same volume

The dynamic analysis result from the same volume variant with force and without force is not having much difference it is cleared from graph 7.6. But the magnet with square cross-section is having a lesser velocity number with force when compared to the same model without force. Another sensitivity analysis was done to conclude that the force is influencing the model to reduce vibration.

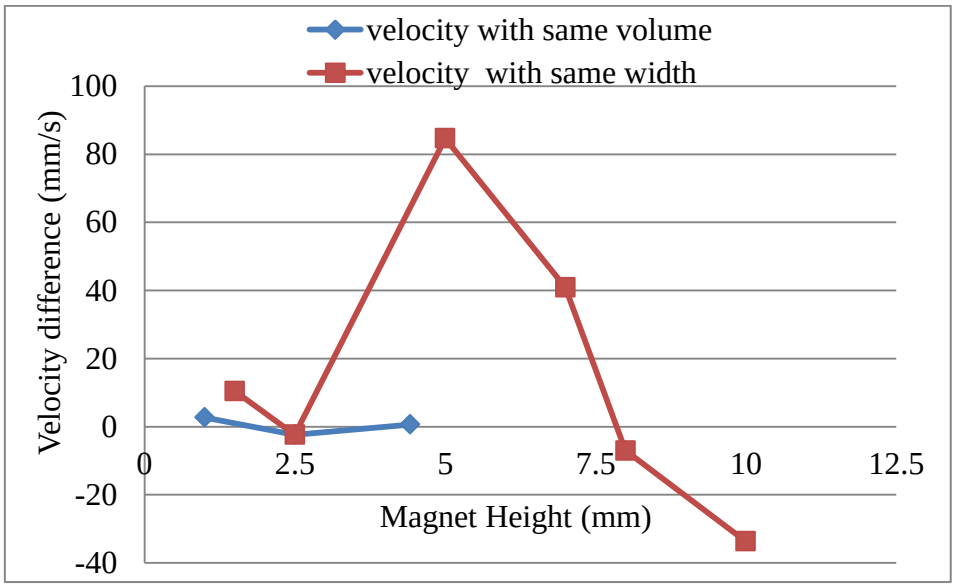

Graph 7.7: Sensitivity analysis of magnets

The sensitivity analysis between velocity differences versus magnet height was done. The velocity difference was calculated by subtracting the maximum velocity value from the model without force to the value with force. The negative velocity difference variant had a force influence on the model. Graph 7.7 shows that a magnet with a square cross-section is

having a negative velocity difference. Also, the magnet with the same volume variant behaves as similar to the same width variant. So bigger magnet will be having better force characteristics, but for the current work with dynamic analysis, it's better to choose a smaller magnet with better force characteristics.

To make sure one more sensitivity analysis was done for a variant of different volumes but having the same width and height cross-section. Along with this, another pair of magnets was analysed with a non-identical magnet, a bigger magnet on the frame, and a smaller magnet on the control part or vice versa. Below table 7.1 demonstrate the value of the velocity for different variant after the first impact between the machine frame and rubber pad.

Magnets dimension	Maximum velocity during impact
20_18_1	421.2998735
20_15_2.5	404.6554
21_15_3	421.9428225
22_15_3.5	454.5548907
28_15_6.5__22_15_2.5	447.7619284
28_15_6.5__20_15_3.5	456.3233117

Table 7.1: Maximum velocity during impact for different square cross-sectioned magnet

Again from this comparison, it was clear that magnets with increasing height had a bigger velocity because of both mass and force influence on the control part. But it is clear from the table that the magnet with a size of 20_15_2.5 is having a lesser velocity than other magnetic pair. So, a dynamic analysis was performed with a square cross-sectioned magnet with a dimension of 20_15_2.5.

The magnetic force act on the control part is equal to the sum of acceleration force and force due to gravity as shown in equation 7.1. By using equation 7.1, a magnetic force for the better vibration Absorber was found which is equal to 1.35 N in its minimum distance between magnets and it was also compared with simulation results from various magnets dynamic analysis (see appendix 6 for calculation part).

$$F_{magnet} = F_{ma} + F_{mg} \tag{7.1}$$

The density of the neodymium magnet is between 7.4-7.5 g/cm^3 that is lesser than the steel 7.8-8.05g/cm^3. So the best variant for the better pair of magnets can be a combination of

maximum use of magnet material on the control part just by replacing the steel material and finding the optimal force value of 1.35N at 3mm distance of magnets. This combination helps to find the better pair of a magnet having the dimension of the outer diameter of 22mm, the inner diameter of 15mm and height of 3.5mm on the control part and outer diameter of 22mm, the inner diameter of 18.75mm and height of 1.25mm on the machine frame for an N52magnets. The velocity value at the impact is around 401.191mm/s which was less when compared to the selected identical magnet of variant having an outer diameter of 20mm, the inner diameter of 15mm, and height of 2.5mm, with the velocity value of 404.6554mm/s. But for the current work, the identical magnet of variant 20_15_2.5 is used by removing excess material on the control part which gives a lesser value of velocity (394.9863mm/s) which is explained later in this chapter.

The dynamic analysis results for various kinematic magnitudes (position, velocity, acceleration) are showed in graphs 7.8 to 7.10. For the analysis comparison magnet was chosen of a square magnet with the same width and height. And the results are compared with the input stroke function. Below graph 7.8 shows the position comparison between input and output of the functional model with a magnet as a modified tool, the blue curve shows the input stroke given to the drive in the model. It already mentioned that the working stroke of the functional model is 32mm it also shown in the graph on the y-axis. And the working period of the complete sewing cycle is 360º (2π), but the motion followed by the upper needle bar to transfer the needle from the upper needle bar to the lower is 60º corresponding to a time of 0.025sec it is mentioned on the x-axis of the curve. The output response was also followed the same curve which is measured on the control part, because of the impact between the machine frame and the rubber pad the curve changes after impact which is shown in the green curve.

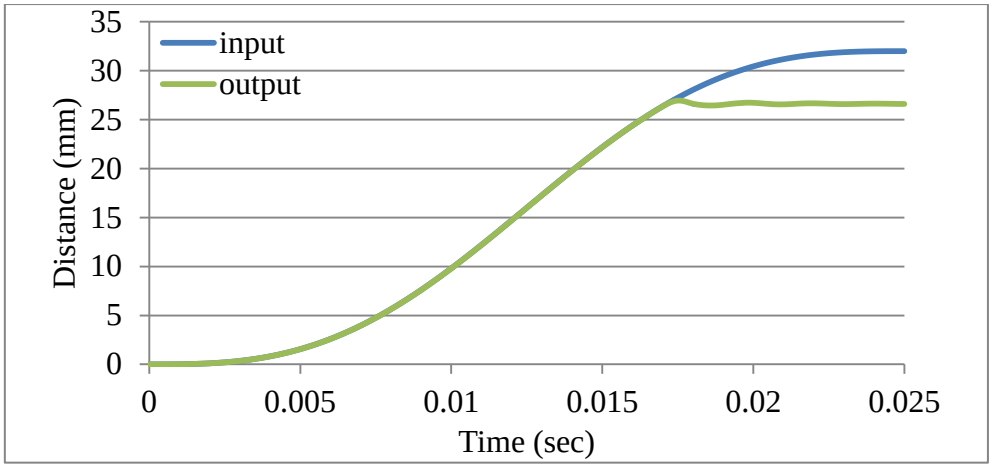

Graph 7.8: Position comparison between input stroke and output response for a modified model with permanent magnets

Graph 7.9 shows the velocity comparison of input function and output response curve for a modified functional model with a permanent magnet. The blue curve represents the input stroke by cycloidal stroke function for an operating speed of 250RPM. The green curve is the response curve from the control part obtained from the model. Curve shows after 0.018sec having vibration oscillation curve this is because of the impact between the machine frame and rubber pad, which is necessary for the needle release mechanism.

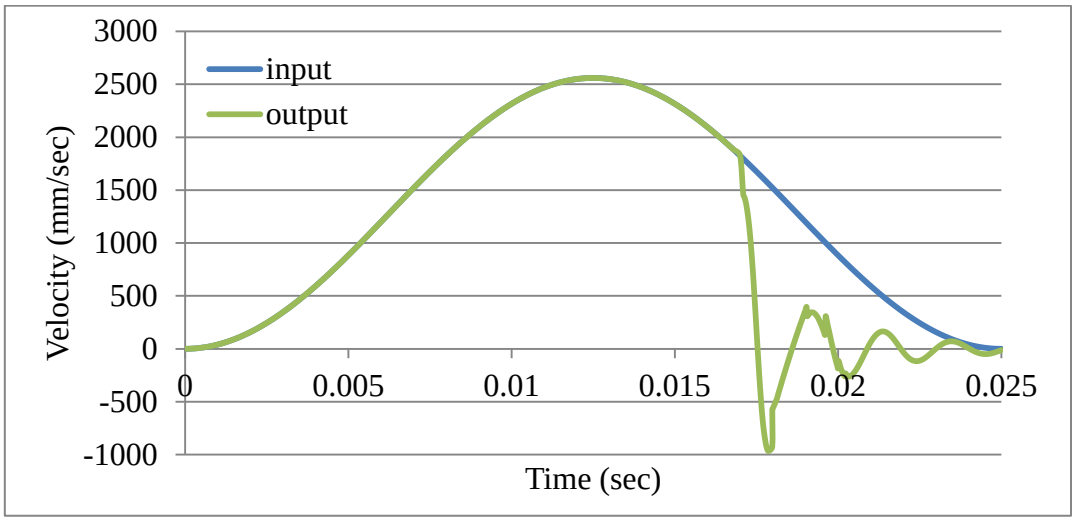

Graph 7.9: Velocity comparison between input stroke and output response for a modified model with permanent magnets

Graph 7.10 shows the acceleration comparison input function and output response curve for the modified functional model with a permanent magnet. The blue curve represents the input stroke by the cycloidal stroke function for an operating speed of 250RPM. The green curve is the response curve from the control part obtained from the model.

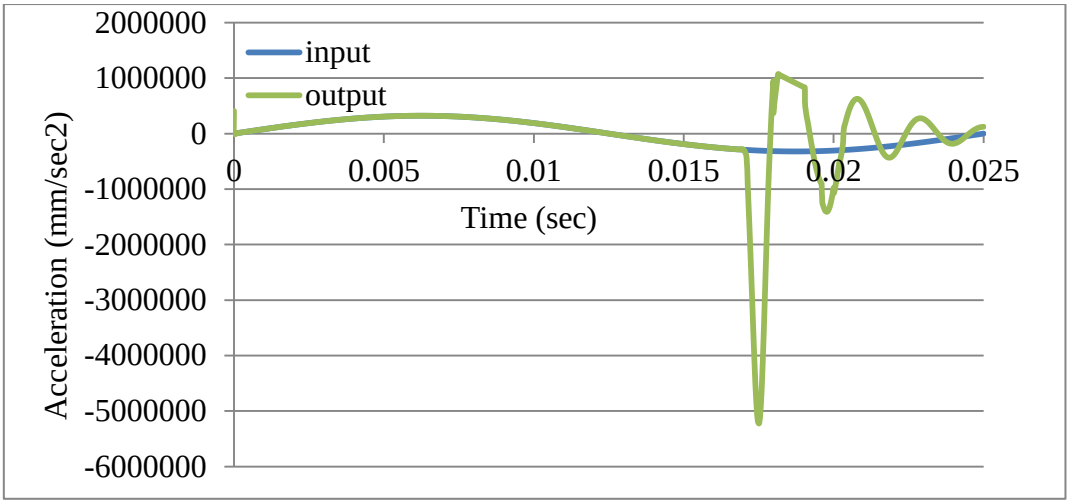

Graph 7.10: Acceleration comparison between input stroke and output response for a modified model with permanent magnets

7.4. Result comparisons

The results obtained from the CREO simulation were transported to an excel sheet to compare the result with input function and output response from an original model without any modification also with a new modified functional model with a permanent magnet below graphs 7.11 to 7.13 show the comparisons between all three curves.

Graph 7.11 shows the Position comparisons between the input function (blue curve) and the output response of the modified functional model with permanent magnets (green curve) also with the functional model without any modification (red curve). From the curve, it has shown that the response of the functional model with modification follows the proper way as a functional model without any modification which is necessary for the functionality of the needle transfer mechanism.

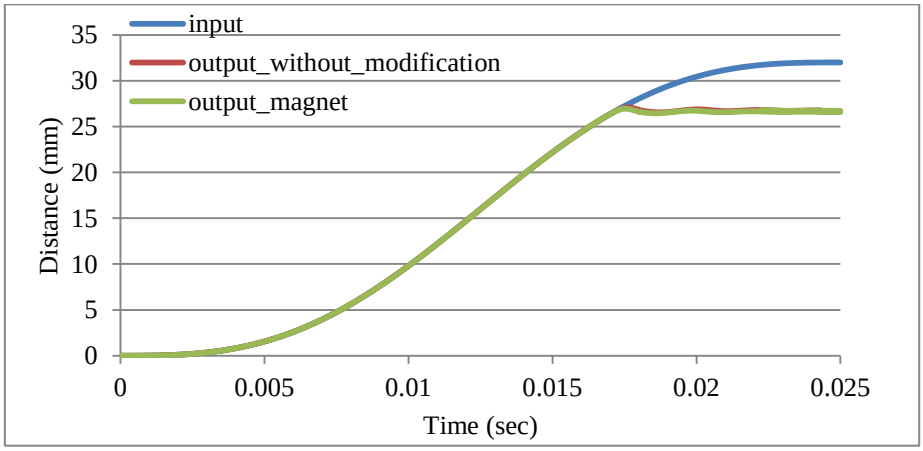

Graph 7.11: Position comparison between input stroke, the output response of the modified model with permanent magnets and with the original unmodified model

The very important parameter to compare the loss of kinetic energy from the model is velocity. Graph 7.12 shows the velocity comparison between all three curves like input function and output response from the functional model with permanent magnet and without any modification to the control part. As explained before there is a vibrational oscillation after the impact of the control part on the rigid frame. In the graph red curve represent the response curve from the control part of the model without any modification had bigger amplitude in velocity when compared to the green curve, which represents the response curve from the control part of the model with a permanent magnet modification.

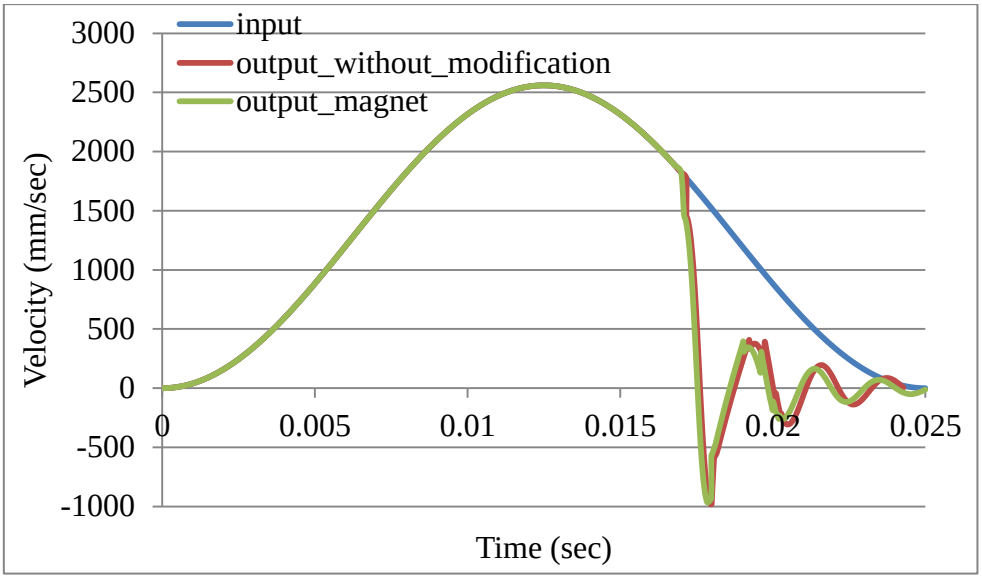

Graph 7.12: Velocity comparison between input stroke, the output response of the modified model with permanent magnets and with the original unmodified model

Sl no	Velocity of the unmodified model (m/s)	Kinetic energy of the unmodified model (J)	Velocity of the modified model (m/s)	Kinetic energy of the modified model (J)
1	0.4073861	0.01681	0.3949863	0.01560

Table 7.2: Kinetic energy comparison between the models

The kinetic energy Table 7.2 shows the velocity value at the time of the impact between the rubber pad and the needle bar machine frame. With the help of the fundamental kinetic energy equation by knowing mass and velocity value at the time of impact loss of kinetic energy was found. It is possible to reduce almost 0.0012J or 1208.58kg.mm^2.s^{-2} energy from the vibration by using permanent magnets as a modification tool. But when compared to compact wire rope isolator the reduction in kinetic energy is very less because of its dynamic behaviour.

The acceleration comparison between input and both the output with the modified functional model with permanent magnet and the functional model without any modification is shown in graph 7.13. As it is seen from the graph the amplitude of the acceleration curve is also reduced drastically as seen in the velocity curve for a modified functional model when compared to the model without any modification.

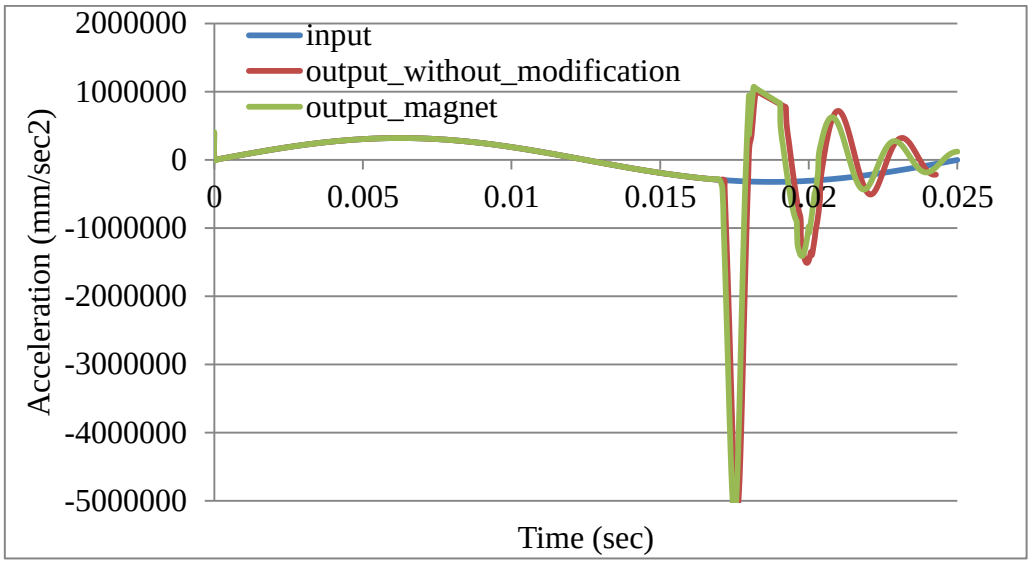

Graph 7.13: Acceleration comparison between input stroke, the output response of the modified model with permanent magnets and with the original unmodified model

The above analysis result and comparison clearly show that with the help of two permanent magnets it is possible to reduce the vibrational loss on the functional model just by using its repulsive force. But the reduction of loss is very much less when compared to another modified method. So the other way of using magnets to reduce the loss of kinetic energy is by modifying the above proposed magnetic vibration absorber which is proposed in appendix 7.

CHAPTER 8. Conclusion and discussion

The dissertation deals with the mechanism of the sewing machine for stitching a decorative stitch using a double-pointed floating needle. During stitching the needle passes through the material and the movement is provided by two mechanical needle bars powered by a synchronous motor through the cam mechanism. The sewing machine is capable of sewing above 500SPM but at this capacity, the system will face a high dynamic load which leads to face high level of vibration, noise, and shock and finally leads to the reduction of productivity. The further study stated that the cam mechanism in the system is the main contributor to vibration and noise generation in the sewing machine (chapter 1 and 2).

Functional model by replacing problematic mechanical cam to electric cam operated by rotary servomotor was done previously. A new functional model was created using a preselected linear servomotor. Design modification was done in such a way that the motion of the needle bar was generated by an individual servomotor. The cycloidal displacement (sinus acceleration) stroke function was used as an input function for dynamic analysis and results for various kinematic magnitudes like position, velocity, and acceleration were produced and compared with it (chapter 3 and 4).

Because of the impact between the rubber pad and the machine frame, there is a loss of kinetic energy in the system. So the main aim of the thesis work is to propose a new modification of the needle bar to eliminate vibrational loss because of impact. By making use of the TRIZ method and basic kinetic energy equation, it was found that the parameters need to control to reduce vibration and noise. 5 different proposal for modification was stated which includes by using Wire rope isolator, permanent magnets, different types of damper, shock-absorbing material, and just by using design modification of needle bar (chapter 5).

In chapter 6, the complete detail about the modification of the needle bar using a compact wire rope isolator (CWRI) was stated. Modification of the design was done by using CREO modelling software then dynamic analysis was conducted by inserting the CWRI characteristics curve into the new modified functional model in the CREO mechanism tool. Later dynamic result for kinematic parameters was generated and compared with the input stroke also with the dynamic results from the unmodified model. It was found that by using CWRI it is possible to reduce 0.0064J or 6426.52kg.mm^2.s^{-2} of kinetic energy which almost equals a 40% reduction in losses (chapter 6).

Chapter 7 deals with the vibration absorber by using two permanent magnets placing like poles facing each other. Firstly the force versus distance characteristics curve was derived by using FEMM 4.2 software for different sized magnets. Secondly, the design modification was done using CREO software. Later the dynamic analysis was done for different variants of the magnet by inserting force characteristics curve to the functional model. Sensitivity analysis was also done from the dynamic result to choose the best pair of magnets to reduce vibrational problems on the functional model. Also with the help of force direction equation and dynamic analysis, the specific force value of 1.35N at 3mm distance was founded, which helps to choose a wide variety of magnetic pair to reduce loss because of impact. It was found that by using two permanent magnets it is possible to reduce 0.0012J or 1208.58kg.mm^2.s^{-2} of kinetic energy which almost equals a 7% reduction in losses (chapter 7).

This thesis work proved that the modification of a needle bar is possible to reduce the kinetic energy loss during the impact of a rubber pad with a needle bar machine frame. The proposed modification with compact wire rope isolator and with the two permanent magnets it is possible to reduce the vibrational loss from an analysis point of view. Again experimental verification is necessary to make a final conclusion to make these proposals suitable for practical application in the real sewing machine. New proposal for MMVA with three magnets was proposed as a future work. Apart from the needle bar, the concept of CWRI and permanent magnet can be used in various fields where vibration and noise are the major issues. Especially, by prolonging the impact time without compromising the functionality of the system.

REFERENCES

[1] *Hand embroidery stitches and stitch families* [online]. Sarah's Hand Embroidery Tutorials. [cit. 15.12.2020]. Available from: https://www.embroidery.rocksea.org/stitch/

[2] *Sewing machine ...The beginning* [online]. Wayback Machine: 2014 [cit. 15.12.2020]. Available from: https://web.archive.org/web/20141220075439/http:/indecohotels.com/sewingmachinebeginning.html

[3] *History of the sewing machine - the birth of mechanical sewing* [online]. Thoughtco: 2019 [cit. 15.12.2020]. Available from: https://www.thoughtco.com/stitches-the-history-of-sewing-machines-1992460

[4] *DECO 2000 - Decorative Hand Stitching Machine* [online]. AMF Reece. [cit. 15,12,2020]. Available from: http://www.amfreece.com/d364-deco-2000.html

[5] PEJCHAR, Karel. *The Analysis and Optimization of the dynamic behaviour of sewing machine DECO 2000*, Diploma work, Liberec, TUL. 2008.

[6] BERAN, Jaroslav, BILEK, Martin, KOMAREK, Jiri, NEMECEK, Pavel. *The Experimental analysis of sewing machine*. MATEC Web of Conferences 89, 01002. 2017.

[7] KOMAREK, Jiri. *The needle bar mechanism of a sewing machine.* Diploma work, Liberec, TUL. 2018.

[8] NORTON, Robert Lioyd. *Design of Machinery, An Introduction to the Synthesis and Analysis of Mechanisms and Machines*. Second edition-2010. ISBN 0-07-048395-7.

[9] KOMAREK, Jiri. *Dynamic model of the Mechanical System of the needle bar*. TUL 2016.

[10] KOMAREK, Jiri, BERAN, Jaroslav, LIMA, Mario, MACHADO, Jose, SILVA, Joao. *Finding the Optimal Setting of the Sewing Needle Transfer Mechanism using Simulation Software*. TUL.

[11] *Linear motors* [online]. Linmot [cit. 25.12.2020]. Available from: https://linmot.com

[12] NORTON, Robert Lioyd. *Cam Design and Manufacturing Handbook*. Second edition-2009. ISBN: 978-0-8311-3367-2

[13] PEJCHAR, Karel, BERAN, Jaroslav. *The Dynamic Analysis of the Needle Bar Mechanism of Sewing Machines*. TUL, 2011, 60-70. ACC_1_07

[14] *TRIZ - A powerful methodology for Creative Problem Solving* [online]. Mindtool [cit. 25.12.2020]. Available from: https://www.mindtools.com

[15] *TRIZ 40 by solid creativity* [online]. TRIZ40 [cit. 25.12.2020]. Available from: http://www.triz40.com

[16] CARVILL, James: *Mechanical engineer's Data Handbook- Thermodynamics and Heat Transfer*, 1994. ISBN: 978-0-7506-1960-8

[17] *Sorbothane – Innovating Shock & Vibration Solutions – Sorbothane overview* [online]. Sorbothane [cit. 25.12.2020]. Available from: https://www.sorbothane.com

[18] BERAN, Jaroslav, PEJCHAR, Karel, Komarek, Jiri. *Analysis and Optimisation of the Needle Transfer Mechanism*. TUL. 2010, 5-12. ACC_1_01

[19] KOMAREK, Jiri. *Influence of the Rubber Pad Stiffness on the Noice of the needle Transfer Mechanism*. TUL

[20] BALAJI, P.S, RAHMAN, M.E, MOUSSA, Leblouba, LAU, H.H. *Wire rope isolators for Vibration isolation of Equipment and Structures – A Review*. IOP Conf. Series: Materials Science and Engineering 78. 2015. doi:10.1088/1757-899X/78/1/012001

[21] RAMIREZ, D.F. Ledezma, NIETO, M. Guzman, GONZALEZ, P.E. Tapia, FERGUSON N.S. *Shock isolation systems using nonlinear stiffness and damping*. ISMA. 2014

[22] FOTI, Francesco, GALEAZZI, Jacopo, MARTINELLI, Luca. *On the Modelling of the Hysteretic Behaviour of Wire Rope Isolators*. XXIV Conference The Italian Association of Theoretical and Applied Mechanics. AIMETA. 2019

[23] RAMIREZ, Diego Francisco Ledezma, GARZA, Fernando Javier Elizondo, GONZALEZ, Pablo Ernesto Tapia, MEDEREZ, Adrian García. *Experimental characterization of dry friction isolators for shock vibration isolation*. 22nd International Congress on Acoustics. 2016

[24] BALAJI, P. S., MOUSSA, Leblouba, RAHMAN, M. E., VUIA, Loo Tshun. *Experimental investigation on the hysteresis behavior of the wire rope isolators*. Journal of Mechanical Science and Technology 29. 2015, 1527-1536. DOI:10.1007/s12206-015-0325-5

[25] *Wire rope isolator, Vibration Isolation Products* [online]. Enidine[cit. 25.12.2020] Available from: http://www.enidine.com/

[26] SAYYAD, F.B, GADHAVE, N.D. *Study of Magnetic Vibration Absorber with Permanent Magnets along with Vibrating Beam Structure*. Hindawi Publishing Corporation Journal of Structures, 658053. 2013, 5 pages. Available from: http://dx.doi.org/10.1155/2013/658053,

[27] YAO, Hongliang, CHEN, Zidong, WEN, Bangchun. *Dynamic Vibration Absorber with Negative Stiffness for Rotor System*. Hindawi Publishing Corporation Shock and Vibration, 5231704. 2016, 13 pages. Available from: http://dx.doi.org/10.1155/2016/5231704,

[28] *Adams Magnetic Products – Neodymium (NdFeB) Magnets* [online]. Adams magnet [cit. 25.12.2020]. Available from: https://www.adamsmagnetic.com

[29] MIYAKE, Takashi, AKAI, Hisazumi. *Quantum Theory of Rare-Earth Magnets*, Journal of the Physical Society of Japan. 2018. Available from: https://doi.org/10.7566/JPSJ.87.041009,

[30] BENACCHIO, S, MALHER, Arnaud, BOISSON, Jean, TOUZE, Cyril. *Design of a Magnetic Vibration Absorber with Tunable Stiffnesses*. IMSIA-France. 2016. Available from: https://hal-ensta.archives-ouvertes.fr/hal-01286056

[31] VALTERA, Jan, SVOBODOVA, Jana, STRNAD, Michal, ZABKA, Petr, KUBE, Vítezslav. *Magnetic accumulation of kinetic energy from a reciprocating mechanical system for a dynamic behaviour improvement*. Journal of Sound and Vibration 451, 2019, 138-146. Available from: https://doi.org/10.1016/j.jsv.2019.03.016

[32] WANG, Shuai, XIN, Wenpen, NING, Yinghao, LI, Bing, HU, Ying. *Design, Experiment, and Improvement of a Quasi-Zero-Stiffness Vibration Isolation System*. Appliedscience 10-2273 MDPI. 2020. Available from: http://dx.doi.org/10.3390/app10072273

APPENDIX 1: New modified functional model with linear servomotor (Manufactured and Assembled model)

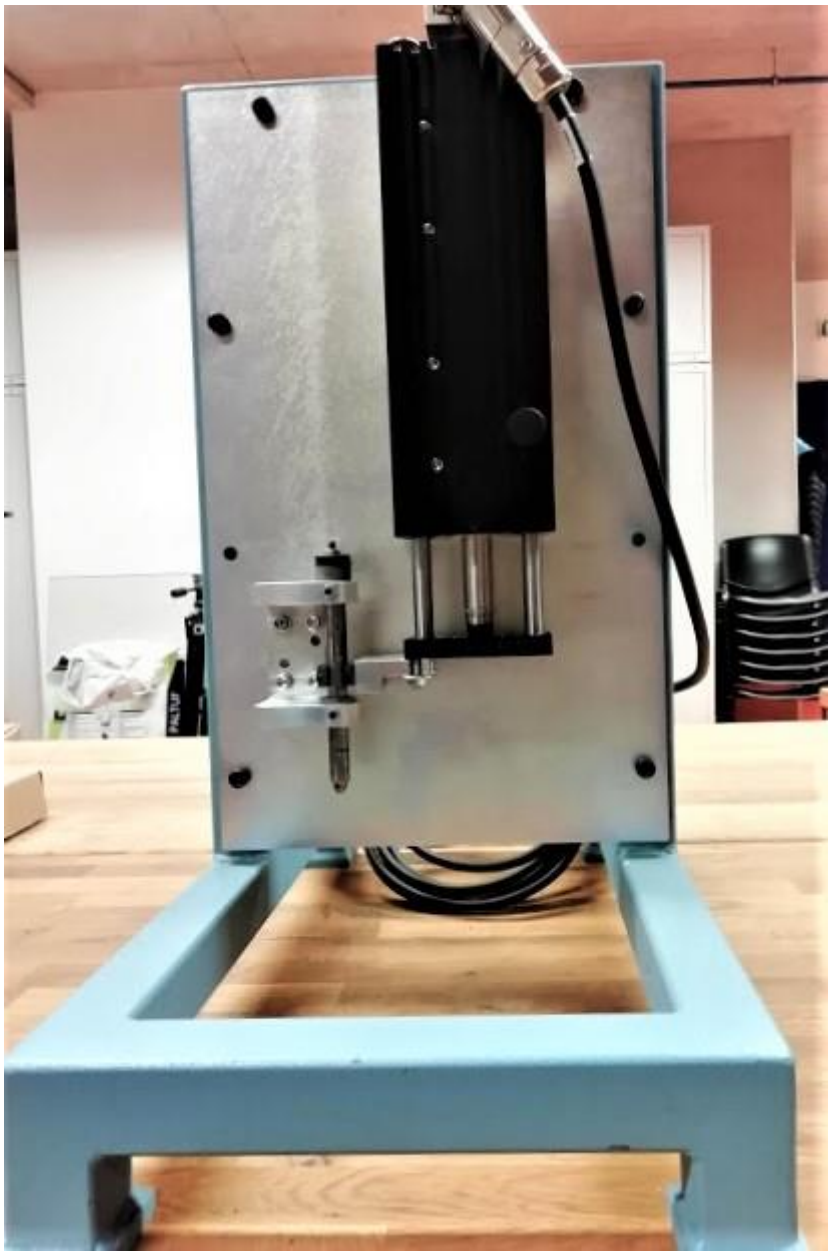

APPENDIX 2: Detailed view of the modified functional model with linear servomotor (Manufactured and Assembled model)

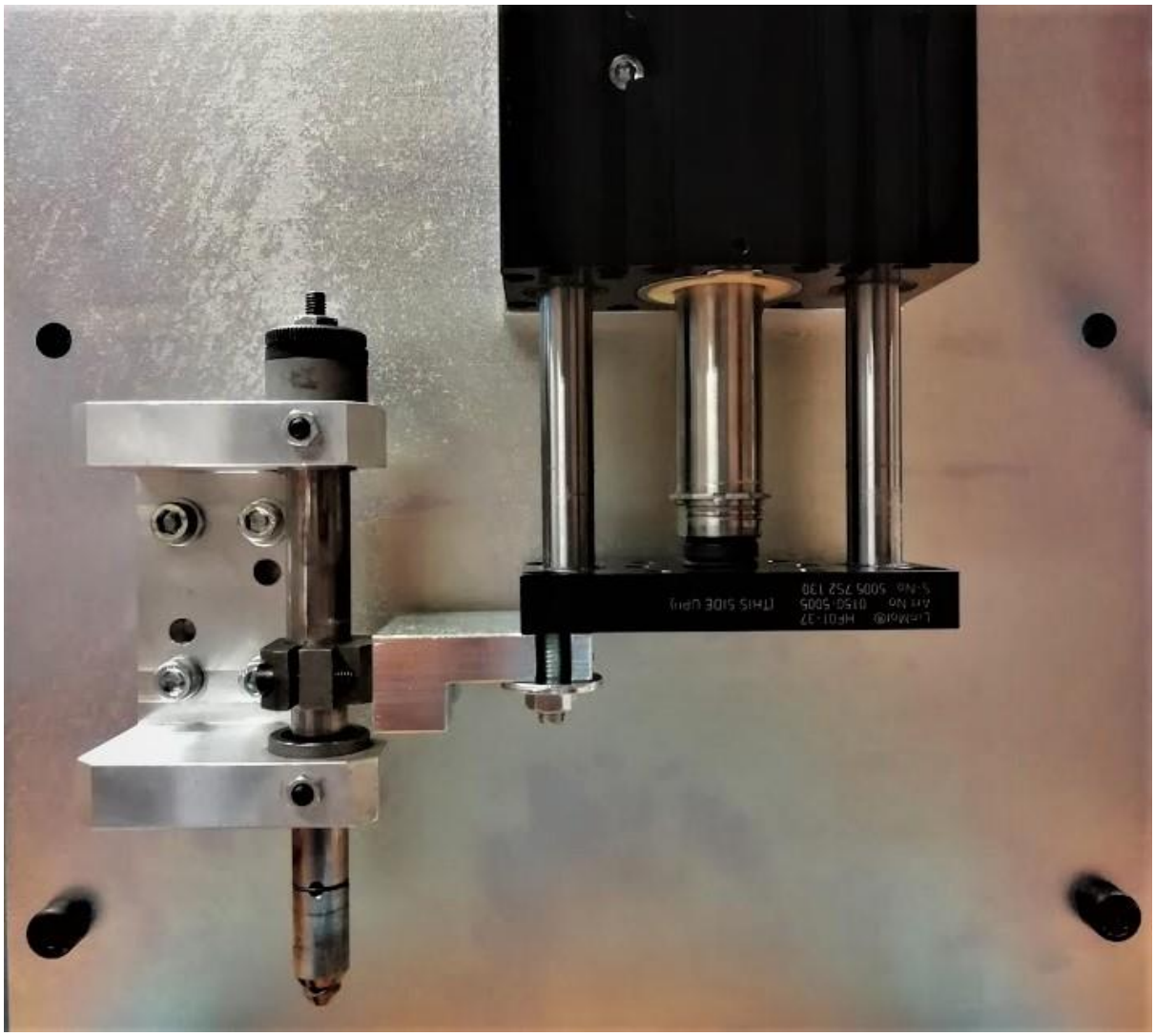

APPENDIX 3: Example of a Lua script written for FEMM 4.2 software to find the Force v/s Distance characteristics curve for a selected magnetic pair.

```
---Heading
Function round(num, idp)
  local mult = 10^(idp or 0)
  return tonumber(format("%." .. (idp or 0) .. "f",
num))
end
```

```
--open("magnetic_spring.FEM")
showconsole()
clearconsole()
--print("setting the initial distance")
newdocument("example.FEM")
--initial setting
mi_probdef(0,'millimeters','axi',1e-15,0,30)
mi_zoom(0,0,15,10)
--material definition
mi_getmaterial("Air")
mi_getmaterial("N35")
-----------------------------Geometry parameters
definition
gr_c=0.01;              --coating thickness - 10um
gr_ra=0.3;              --function edges radius
gr_rb=0.3;              --other edges radius
gr_areaR = 60           --surroundings simulation area
size
si_step = 1;            --step of the simulation
stepsize_1=1.5;         -- simulation step - coarse
stepsize_2=2;           -- simulation step - medium
stepsize_3=1;           -- simulation step - fine
limit_1=3;              -- limit 1
limit_2=9;              -- limit 2
limit_0=40;             -- limit 3
nsteps=limit_2/stepsize_3+(limit_1-
limit_2)/stepsize_2+(limit_0-limit_1)/stepsize_1;
-------------------------------------------------
geometry - magnet static
d1 = 20/2+gr_c;         --d inner diameter (mm)
D1 = 15/2-gr_c;         --D outer diameter (mm)
h1 = 2.5-gr_c;          --h inner height (mm)
H1=h1;                  --H outer height (mm)
gr_magMaterial1 = 'N35 -- selection of required material
s1 = -0.3;              -- minimal gap
-------------------------------------------------------
geometry - magnet moving
d3 = 20/2+gr_c;         --d inner diameter (mm)
D3 = 15/2-gr_c;         --D outer diameter (mm)
h3 = 2.5-gr_c;          --h inner heigth (mm)
```

```
H3=h3;                  --H outer height (mm)
gr_magMaterial3 = 'N35';--selection of required material
s3 = 0.0;               -- initial distance of magnets
-----------------------------------------------------
gr_name="mag_base";
gr_num=1;
-----------definition of points (x,y - coordinates),
group selection
gr_BodyX={d1,D1,D1,d1}
gr_BodyY={h1,H1,0,0}
for n=1,4,1 do
  print(gr_BodyX[n])
  mi_addnode(gr_BodyX[n],gr_BodyY[n])
  mi_selectnode(gr_BodyX[n],gr_BodyY[n])
  mi_setnodeprop(gr_name,gr_num)
end
-----------definiton of lines
for n=1,4,1 do
  print(gr_BodyX[n])
  m=n
  if m==4 then m=0 end

mi_addsegment(gr_BodyX[n],gr_BodyY[n],gr_BodyX[m+1],gr_B
odyY[m+1])

mi_selectsegment((gr_BodyX[n]+gr_BodyX[m+1])/2,(gr_BodyY
[n]+gr_BodyY[m+1])/2)
    mi_setsegmentprop(gr_name,1,0,0,gr_num)
end
-----------edge radius definition
     mi_createradius(gr_BodyX[1],gr_BodyY[1],gr_ra);
     mi_createradius(gr_BodyX[2],gr_BodyY[2],gr_ra);
     mi_createradius(gr_BodyX[3],gr_BodyY[3],gr_rb);
     mi_createradius(gr_BodyX[4],gr_BodyY[4],gr_rb);
-----------material block definition
mi_addblocklabel((gr_BodyX[2]-
gr_BodyX[1])/2+gr_BodyX[1],(gr_BodyY[1]-
gr_BodyY[4])/2+gr_BodyY[4])
mi_selectlabel((gr_BodyX[2]-
gr_BodyX[1])/2+gr_BodyX[1],(gr_BodyY[1]-
gr_BodyY[4])/2+gr_BodyY[4])
```

```
mi_setblockprop(gr_magMaterial1,0,0,'<None>','90',gr_num
,0);
-----------------------------------------------------
moving magnet definition
gr_name="mag_move";
gr_num=3;
-----------definition of points (x,y - coordinates),
group selection
gr_BodyX={d3,D3,D3,d3}
gr_BodyY={s1+h1+h3+s3+2.83,s1+h1+s3+h3+2.83,s1+s3+h1+2.8
3,s1+s3+h1+2.83}
for n=1,4,1 do
  print(gr_BodyX[n])
  mi_addnode(gr_BodyX[n],gr_BodyY[n])
  mi_selectnode(gr_BodyX[n],gr_BodyY[n])
  mi_setnodeprop(gr_name,gr_num)
end
-----------definiton of lines
for n=1,4,1 do
  print(gr_BodyX[n])
  m=n
  if m==4 then m=0 end

mi_addsegment(gr_BodyX[n],gr_BodyY[n],gr_BodyX[m+1],gr_B
odyY[m+1])

mi_selectsegment((gr_BodyX[n]+gr_BodyX[m+1])/2,(gr_BodyY
[n]+gr_BodyY[m+1])/2)
    mi_setsegmentprop(gr_name,1,0,0,gr_num)
end
-----------edge radius definition
     mi_createradius(gr_BodyX[1],gr_BodyY[1],gr_ra);
     mi_createradius(gr_BodyX[2],gr_BodyY[2],gr_ra);
     mi_createradius(gr_BodyX[3],gr_BodyY[3],gr_rb);
     mi_createradius(gr_BodyX[4],gr_BodyY[4],gr_rb);
-----------material block definition
mi_addblocklabel((gr_BodyX[2]-
gr_BodyX[1])/2+gr_BodyX[1],(gr_BodyY[1]-
gr_BodyY[4])/2+gr_BodyY[4])
mi_selectlabel((gr_BodyX[2]-
gr_BodyX[1])/2+gr_BodyX[1],(gr_BodyY[1]-
gr_BodyY[4])/2+gr_BodyY[4])
```

```
mi_setblockprop(gr_magMaterial3,0,0,'<None>','270',gr_nu
m,0);
----------------------------------------surrounding area
definition
gr_name="area";
----------definition of points (x,y - coordinates),
group selection
gr_num=9;
gr_BodyX = {0,0}
gr_BodyY= { -gr_areaR,gr_areaR}              --
definition of the area for simulation
mi_addnode(gr_BodyX[1],gr_BodyY[1])
mi_selectnode(gr_BodyX[1],gr_BodyY[1])
mi_setnodeprop(gr_name,gr_num)
mi_addnode(gr_BodyX[2],gr_BodyY[2])
mi_selectnode(gr_BodyX[2],gr_BodyY[2])
mi_setnodeprop(gr_name,gr_num)
----------definiton of lines, segments
mi_addsegment(gr_BodyX[1],gr_BodyY[1],gr_BodyX[2],gr_Bod
yY[2])
mi_selectsegment(gr_BodyX[1],gr_BodyY[2]+gr_BodyY[1])
mi_setsegmentprop(gr_name,1,0,0,gr_num)
mi_addarc(gr_BodyX[1],gr_BodyY[1],gr_BodyX[2],gr_BodyY[2
],180,1)
----------material block definition
mi_addblocklabel(10,gr_areaR*0.8)
mi_selectlabel(10,gr_areaR*0.8)
mi_setblockprop('Air',0,0,'<None>',0,0,0);
----------boundary condition definition
bo_name = "outer";
bo_c0 = 0;
bo_c1 = 0;
bo_BdryFormat = 1; --0=fixed voltage, 1=mixed, 2=surface
charge density, 3=priodic, 4=anti-periodic
mi_addboundprop(bo_name, 0, 0, 0, 0, 0, 0, bo_c0, bo_c1,
BdryFormat)
mi_selectarcsegment(gr_BodyX[1],gr_BodyY[1])
mi_setarcsegmentprop(1,bo_name,0,gr_num)
----------------------------------------------------
program
showconsole()
```

```
clearconsole()
distance=s3;
mi_saveas("temp.FEM")
for n=1,nsteps,1 do --loop shifting the geometry with
the stepzise 1
     if (n>1) then
          if (distance>limit_0) then
          mi_close() --close the solution
          else
               if (distance>limit_2) then
               si_step=stepsize_3;
               else
                    if (distance>limit_1) then
                    si_step=stepsize_2;
                         else
                         si_step=stepsize_1;
                         end
               end
          end
mi_seteditmode("group")    --group editing
mi_selectgroup(3)          --selection of the group nu 3
mi_movetranslate(0,si_step,4)--move it in Y coordinate
of 1 step
mi_selectgroup(4)           --selection of the group nu 4
mi_movetranslate(0,si_step,4)--move it in Y coordinate
of 1 step
distance=distance+si_step;-- increase the distance value
by the step
   end
mi_analyze()
mi_loadsolution()
--show solution
mo_showdensityplot(1,0,2,0,"bmag")--show the map of
field density
mo_groupselectblock(1)
ffx=mo_blockintegral(19)--weighted stress tensor
print(0,round(1*distance,1),round(-1*ffx,2))--show the
console with distance and force value
end
```

APPENDIX 4: Magnetic analysis result obtained from the FEMM 4.2 software for a written script.

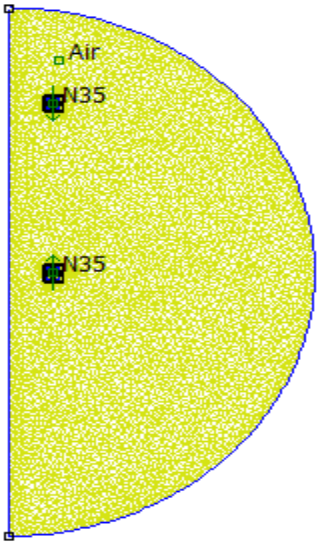

Model in the FEM view

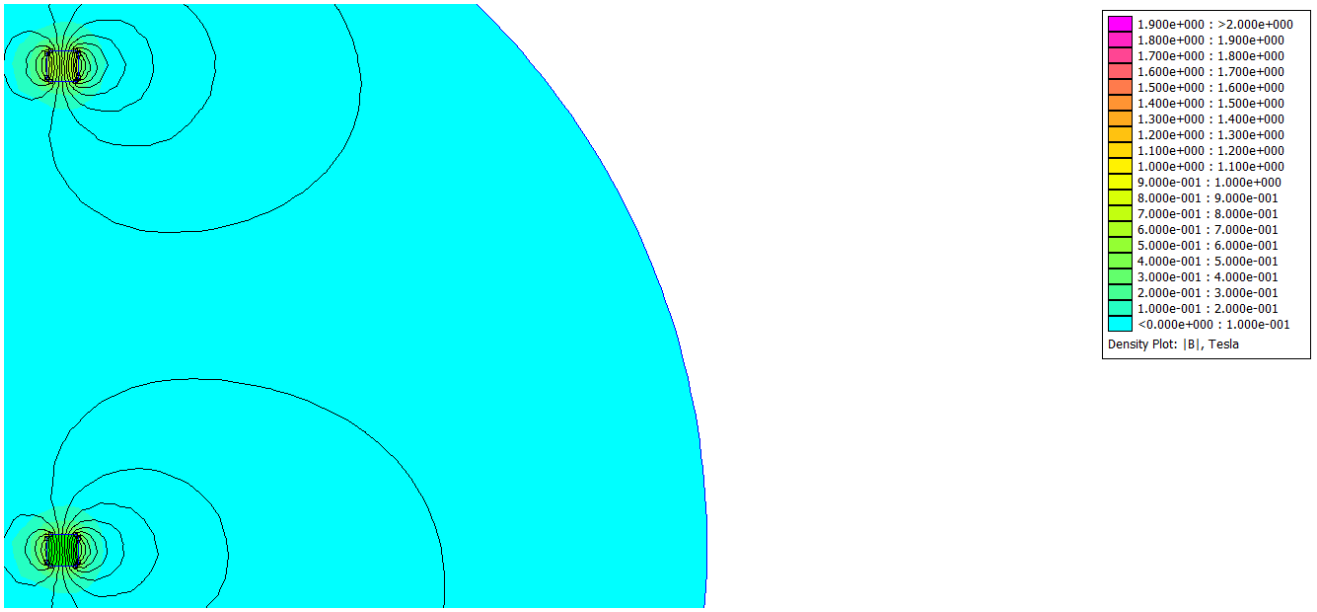

Magnetic Field result for a pair of selected magnet

APPENDIX 5: Critical damping value calculation for compact wire rope isolator.

Maximum deflection (x): 0.003m

Maximum force acting (F): 24N

$\therefore$ Maximum stiffness (k) = $\frac{F}{x} = \frac{24}{0.003}$=8000 N/m

Maximum acceleration (a): 1.07 x 10^3 m/sec^2

Net force act on the WRI is $Fnet = F_{ma}+F_{mg}$

$$F=ma + mg$$

$$F=m\,(a+g)$$

$\therefore$ Mass of the control part (m)= $\frac{F}{(a+g)}=\frac{24}{1079.81}$ =0.0222 + 0.0028=0.025kg

$\therefore$ Critical damping value for a WRI (C_c) = $2\sqrt{km}$= 26.7 Ns/m

The above find critical value is for maximum value. The WRI is having non-linear behaviour the value is not the same in all points. For the minimum force and deflection values, the damping value is above 50 Ns/m. So for the dynamic analysis, an estimated value of damping was used from a critical damping calculation and from the previous damping value used in a model which is around 30Ns/m.

APPENDIX 6: Magnetic force calculation

From equation 7.1, it is possible to estimate the better magnetic force at the distance of 3mm (because the rubber pad is having a thickness of 3mm) can be used for the model to observe kinetic energy.

$$F_{magnet} = F_{ma} + F_{mg}$$

Since acceleration varies to time and due to the limitation of software the magnetic force at the distance of 3mm is finding as an ideal value at the time of impact. The acceleration force at the time of the first impact is big and negative. So equation 7.1 become,

$$\therefore F_{magnet}+F_{ma} = F_{mg}=1.96\text{N}$$

Assumption:

1. Mass is a needle bar (200g) was considered for this calculation.
2. But bigger magnetic force affect the functionality so by eliminating acceleration force from the above equation it can be rewrite as,

$$F_{magnet} < F_{mg}$$

After a series of dynamic analyses, the value of magnetic force was set as 1.35N for the modified functional model and it will vary according to the functionality of the model.

APPENDIX 7: Proposed Modified Magnetic Vibration Absorber

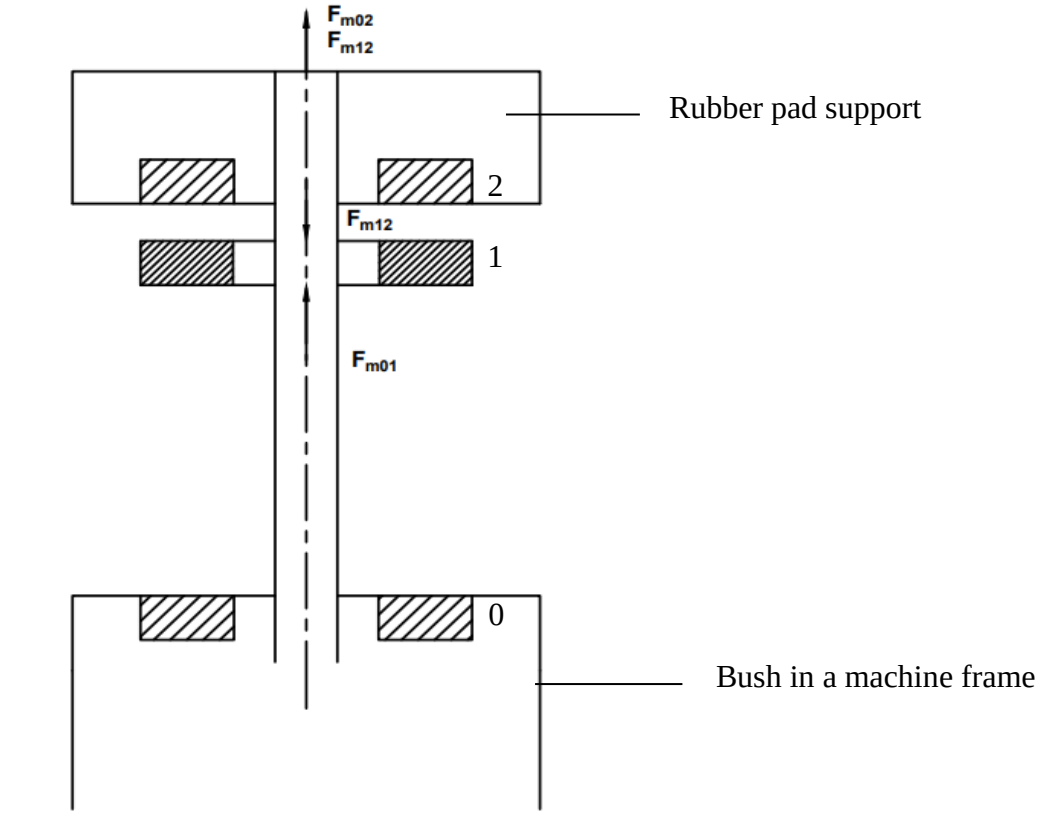

The modified new proposal is made up of three magnets in which the first two magnets (0 and 1) facing like pole each and above two magnet facing opposite poles each other (1and 2). Because of the fixed rubber pad, there will constant attraction force between magnets 1 and 2 also there is an additional repulsive force between magnets 0 and 1 along with the previous repulsive force first and last magnet (0 and 2).

APPENDIX 8: Drawing documentation

Drawing documentation is in the separate binding book, according to the following order;

SL.No.	Drawing Name	Drawing Number
1	FUNCTIONAL_MODEL_WRI	KTS1_0_00_FUNCTIONAL_MODEL
2	SUPPORT_PLATE	KTS1_0_01_ SUPPORT_ PLATE
3	SPACER _PLATE	KTS1_0_02_ SPACER _PLATE
4	CONNECTING_PART	KTS1_0_03_ CONNECTING_PART
5	FUNCTIONAL_MODEL_MAGNET	KTS2_0_00_FUNCTIONAL_MODEL
6	SUPPORT_PLATE	KTS2_0_01_ SUPPORT_PLATE
7	SPACER _PLATE	KTS2_0_02_ SPACER _PLATE
8	CONNECTING_PART	KTS2_0_03_ CONNECTING_PART
9	RUBBER_PAD_SUPPORT	KTS2_0_04_ RUBBER_PAD_SUPPORT
10	BLOCK_BUSH	KTS2_0_05_ BLOCK_BUSH